Characterization of Phagosome Trafficking and Identification of PhoP-Regulated Genes Important for Survival of *Yersinia pestis* in Macrophages†

Jens P. Grabenstein,‡ Hana S. Fukuto, Lance E. Palmer, and James B. Bliska*

Department of Molecular Genetics and Microbiology and Center for Infectious Diseases,
SUNY at Stony Brook, Stony Brook, New York 11794-5222

The transcriptional activator PhoP is important for survival of *Yersinia pestis* in macrophage phagosomes. However, the phagosomes inhabited by *Y. pestis* have not been well characterized, and the mechanism by which PhoP promotes bacterial survival in these vacuoles is not fully understood. Lysosomal tracers, as well as antibodies to late endosomal or lysosomal proteins, were used in conjunction with confocal or electron microscopy to study the trafficking of phagosomes containing *phoP*⁺ or *phoP* mutant *Y. pestis* strains or latex beads in J774A.1 macrophages. Phagosomes containing *phoP*⁺ or *phoP* mutant *Y. pestis* acquired lysosomal markers to the same degree that phagosomes containing latex beads acquired these markers after 1.5 h of infection, showing that nascent phagosomes containing *Y. pestis* fuse with lysosomes irrespective of the *phoP* genotype. Similar results were obtained when phagosomes containing viable or dead *phoP*⁺ *Y. pestis* cells or beads were analyzed at 8 h postinfection, indicating that the *Y. pestis* vacuole does not become secluded from the lysosomal compartment. However, only viable *phoP*⁺ bacteria induced the formation of spacious phagosomes at 8 h postinfection, suggesting that *Y. pestis* can actively direct the expansion of its vacuole. PhoP-regulated genes that are important for survival of *Y. pestis* in phagosomes were identified by Tn5-*lacZ* mutagenesis and oligonucleotide microarray analysis. Three such genes were identified, and the products of these genes are predicted to promote resistance to antimicrobial peptides (*ugd* and *pmrK*) or low-Mg²⁺ conditions (*mgtC*) found in phagosomes. Viable count assays carried out with *Y. pestis ugd*, *mgtC*, and *ugd mgtC* mutants revealed that the products of *ugd* and *mgtC* function independently to promote early survival of *Y. pestis* in macrophage phagosomes.

Yersinia pestis is a gram-negative bacterium and the causative agent of bubonic, septicemic, and pneumonic plague (56). Zoonotic foci of plague exist in many parts of the world, including North America. Most commonly, *Y. pestis* infections are transmitted to humans by infected fleas, and these infections typically develop into bubonic plague or, less frequently, into septicemic plague (56). Plague infections in humans can also result from contact with body fluids or from inhalation of respiratory droplets from infected animals or humans. Inhalation of *Y. pestis* into the lungs can initiate an infection known as primary pneumonic plague. Pneumonic plague follows a more rapid course and has a higher mortality rate than bubonic or septicemic plague. These characteristics make development of plague into a biological weapon possible and have led to designation of *Y. pestis* as a Category A agent (36).

Y. pestis is a facultative intracellular pathogen that is able to survive and replicate inside macrophages in vitro (11, 12, 37, 58, 66). Microscopic examination of tissues of animals experimentally infected with *Y. pestis* has shown the presence of plague bacilli inside macrophages (21, 45, 70). More often,

however, large numbers of *Y. pestis* cells replicating extracellularly in tissues are detected (40, 64, 71). *Y. pestis* produces several antiphagocytic factors that are upregulated during growth at 37°C. These factors include several Yop proteins and their designated type III secretion system (TTSS) encoded on pCD1 (69). In addition, a capsule composed of the F1 protein is maximally expressed after extended growth at 37°C and promotes resistance to phagocytosis (17). When grown at ambient temperatures (e.g., 28°C), *Y. pestis* is efficiently phagocytosed by macrophages (11). For these reasons it has been hypothesized that when *Y. pestis* is introduced into a host, it initially survives and replicates within macrophages that internalize the bacteria (11). Subsequently, the bacteria are released from macrophages and replicate extracellularly as a consequence of upregulation of antiphagocytic factors (11). However, recently Lukaszewski et al. reported that a large percentage of *Y. pestis* bacteria are inside spleen macrophages in mice during the first several days of infection (43). The extent to which *Y. pestis* exists within macrophages during infection in vivo may depend on the nature of the host, the temporal stage of the infection, and the specific tissue infected.

Pathogenic bacteria that survive within macrophages utilize different strategies to avoid being killed in a vacuole that could potentially mature into a phagolysosome (18). For example, *Salmonella enterica* serovar Typhimurium is internalized into a macrophage vacuole that may initially fuse with lysosomes (14, 52). However, within several hours, *S. enterica* serovar Typhimurium modifies the vacuole into a specialized compartment

---

* Corresponding author. Mailing address: Department of Molecular Genetics and Microbiology and Center for Infectious Diseases, SUNY at Stony Brook, Stony Brook, NY 11794-5222. Phone: (631) 632-8782. Fax: (631) 632-9797. E-mail: jbliska@ms.cc.sunysb.edu.
† Supplemental material for this article may be found at http://iai.asm.org/.
‡ Present address: New York University School of Medicine, 550 First Avenue, New York, NY 10016.

TABLE 1. *Y. pestis* strains used in this study

Strain	Relevant characteristics	Reference
KIM10+*phoP*Δ	Biovar Mediaevalis, pCD1−, pPCP1−, *phoP*Δ127-429	25
KIM10+*phoP*Δ/MMB67EH	KIM10+*phoP*Δ, pMMB67EH, Ap^r	25
KIM10+*phoP*Δ/PhoP	KIM10+*phoP*Δ, pPhoP, Ap^r	25
KIM10+*phoP*Δ/PhoP2	KIM10+*phoP*Δ, pPhoP2, Cm^r	This study
KIM6+	Biovar Mediaevalis, pCD1−	24
KIM6+*phoP*Δ	KIM6+*phoP*Δ127-429	This study
KIM6+*ugd*Δ	KIM6+*ugd*Δ651-911	This study
KIM6+Δ*pmrF*::*kan*	KIM6+*pmrF*Δ15-833Ω*aphA-3*, Kn^r	This study
KIM6+*pagP*::*kan*	KIM6+*pagP*::*kan*, Kn^r	This study
KIM6+*mgtC*::*kan*	KIM6+*mgtC*::*kan*, Kn^r	This study
KIM6+*y2124*::*kan2*	KIM6+*y2124*::*kan2*, Kn^r	This study
KIM6+*y2816*::*kan2*	KIM6+*y2816*::*kan2*, Kn^r	This study
KIM5/GFP	KIM6/pCD1Ap, pMMB207gfp3.1, Ap^r Cm^r	This study
KIM5*phoP*Δ/GFP	KIM6 *phoP*Δ127-429, pCD1Ap, pMMB207gfp3.1, Ap^r Cm^r	This study
KIM6+/PGFP	KIM6+, pMMB207pgfp3.1, Cm^r	This study

that becomes secluded from the lysosomal compartment (14, 35, 39, 60). The macrophage vacuole inhabited by *Y. pestis* has not been well characterized, but there is some evidence that there is fusion of lysosomes with the *Y. pestis*-containing phagosome at early infection times. Straley and Harmon found that after a 1-h infection *Y. pestis*-containing phagosomes had fused with lysosomes preloaded with thorium dioxide (67). In another study the workers used acridine orange as a lysosomal tracer and reported that the vast majority of *Y. pestis*-containing phagosomes had fused with preformed lysosomes after 2.5 h of infection (12). These studies indicate that the nascent *Y. pestis*-containing vacuole is competent for fusion with lysosomes, but it is not known if the phagosome becomes secluded from the lysosomal compartment at later infection times, as it does in the case of *S. enterica* serovar Typhimurium.

Several studies have investigated the genetic basis of the ability of *Y. pestis* to survive and replicate within macrophages. Straley and Harmon showed that pCD1 and pPCP1 were not required for replication in murine macrophages (66). It was also reported that strains lacking the pigmentation (*pgm*) locus, due to spontaneous deletion of the 102-kbp chromosomal region, are able to replicate in naïve macrophages (66). Recently, it has been shown that *rip* genes in the *pgm* locus are required for survival of *Y. pestis* in activated macrophages (59). The *phoP* gene, which encodes a transcriptional activator, is important for survival of *Y. pestis* in macrophages (25, 54). In *S. enterica* serovar Typhimurium PhoP induces gene expression under low-Mg^{2+} conditions or in response to cationic antimicrobial peptides in vitro, and under normal conditions it requires the sensor kinase PhoQ to be activated (2, 19, 26). In phagosomes, PhoP appears to be positively regulated by antimicrobial peptides, acidification, and/or low-Mg^{2+} conditions, as well as by other uncharacterized signals (19, 26, 53). The PhoP-regulated genes important for survival of *S. enterica* serovar Typhimurium in the phagosome include genes of the *pmr* operon. The products of the *pmr* operon modify lipid A with aminoarabinose, and this increases bacterial resistance to antimicrobial peptides (19, 26). In *S. enterica* serovar Typhimurium PhoP does not directly activate transcription of the *pmr* operon in response to a low Mg^{2+} concentration. Instead, PhoP activates expression of *pmrD*, which encodes a posttranscriptional activator of PmrA, a second two-component tran-

scriptional activator (26). Once activated, PmrA binds to the *pmr* promoter and activates expression of the operon (26). In *Y. pestis*, PhoP has been shown to be activated by low-Mg^{2+} conditions and to positively regulate a number of genes homologous to genes found in *S. enterica* serovar Typhimurium, including a *pmr*-like operon (33, 61, 72, 73). However, it is not known which PhoP-regulated genes are important for survival of *Y. pestis* in macrophages.

In this study we analyzed the trafficking of the *Y. pestis*-containing vacuole in macrophages to obtain a better understanding of the intracellular environment in which the bacterium survives. We present evidence showing that *Y. pestis* resides in a vacuole that undergoes fusion with lysosomes and does not become secluded from the lysosomal pathway during the first 8 h of infection. In addition, we identified a subset of PhoP-regulated genes that are important for survival of *Y. pestis* in the hostile phagosome environment.

MATERIALS AND METHODS

Antibodies. The primary antibodies used were a polyclonal rabbit anti-*Yersinia* antibody designated SB349 (5) diluted 1:1,000, a polyclonal rabbit anti-cathepsin D antibody (Scripps Laboratories) diluted 1:200, and a monoclonal rat anti-Lamp1 antibody (1D4B; Developmental Studies Hybridoma Bank, University of Iowa) diluted 1:50. The secondary antibodies used were goat anti-rabbit antibodies conjugated to Alexa-594 or Alexa-633 and a goat anti-rat antibody conjugated to Alexa-647 purchased from Molecular Probes.

Bacterial strains and growth conditions. The *Y. pestis* strains used in this study are listed in Table 1. *Y. pestis* strains were cultivated at 28°C on heart infusion (HI) (Difco) or Luria-Bertani (LB) agar plates. Cultures were grown in HI broth with aeration overnight at 28°C. The growth medium for *Y. pestis* was supplemented with 25 μg/ml ampicillin, 25 μg/ml kanamycin, 10 μg/ml chloramphenicol, 25 μg/ml spectinomycin, 25 μg/ml streptomycin, or 20 μg/ml tetracycline when appropriate. *Escherichia coli* strains NovaBlue (Novagen), SM10, and S17-1, which were used for plasmid and mutant construction, were grown as described previously (25).

Construction of KIM6+ mutants. PCRs, T4 polymerase reactions, DNA ligation, DNA restriction, and DNA cycle sequencing reactions were carried out as described previously (25). Genes or open reading frames (ORFs) used for mutational inactivation were amplified by PCR using appropriate primers (see Table S1 in the supplemental material), inserted into the EcoRV site of the pETBlue-2 cloning vector using a Perfectly Blunt cloning kit (Novagen), and sequenced using previously described methods (25). The resulting plasmids were subjected to in vitro transposon mutagenesis to create insertions in ORFs (y2124 and y2816) using an EZ::TN <KAN-2> transposon kit (Epicenter). Alternatively, the kanamycin resistance cassette (*kan*) from plasmid pBSL86 (1) was excised by restriction digestion, gel purified, and inserted into the appropriate

target gene (*pagP* or *mgtC*) by ligation. For *pagP* the *kan* cassette was inserted into the MfeI site, and for *mgtC* the *kan* cassette was inserted into the SacII site. The genes or ORFs containing the *kan* cassette or the *kan-2* transposon were inserted into suicide vector pSB890 (25) using either BamHI (y2124, y2816, and *pagP*) or SmaI (*mgtC*) restriction sites. To create an in-frame deletion mutation in *ugd*, pETBlue-2 plasmid DNA containing *ugd* was digested with HpaI and SphI to remove nucleotides 651 to 911 of the *ugd* sequence. After restriction digestion, a T4 DNA polymerase reaction was performed to create blunt ends, and the blunt ends were ligated to create pETBlue-2*ugd*Δ. A BamHI restriction fragment containing *ugd*Δ was excised from pETBlue-2 and inserted into the BamHI site of suicide vector pSB890. A derivative of pSB890 used to construct an in-frame deletion in *phoP* has been described previously (25). The different *kan* insertion or unmarked deletion mutations carried by the pSB890 plasmids were introduced into KIM6+ using allelic recombination as described previously (25). The Δ*pmrF*::*kan* mutation was introduced into KIM6+ by allelic exchange using the pMRF1 plasmid (44).

Construction of GFP expression plasmids. The *gfpmut3.1* gene was isolated from pGFPmut3.1 (Clontech) and inserted between the HindIII and XbaI sites of pMMB207 (49), resulting in pMMB207gfp3.1. This plasmid expresses green fluorescent protein (GFP) under control of the *tac* promoter. To place *gfp* expression under control of the *ugd* promoter, the promoter region of *ugd* (positions −434 to 30) was amplified by PCR using primers Y2147P1F and Y2147P1R (see Table S1 in the supplemental material). The primers were designed to create an XmaI site at the 5' end and an SphI site at the 3' end of the PCR product. The DNA product was digested with XmaI and SphI and inserted into the XmaI and SphI sites of pMMB207gfp3.1, resulting in pMMB207pgfp3.1. Plasmids pMMB207gfp3.1 and pMMB207pgfp3.1 were introduced into S17λpir and then conjugated into KIM6+. The resulting strains were designated KIM6+/GFP and KIM6+/PGFP, respectively (Table 1).

Construction of *Y. pestis* KIM5(pCD1Ap) strains. Overnight cultures of KIM6+/GFP and KIM6+*phoP*Δ/GFP were diluted in HI broth and plated on Congo red plates (20) to identify colonies that had lost the pigmentation (*pgm*) locus by spontaneous deletion. Nonpigmented colonies were picked and streaked on Congo red and *Yersinia* selective medium (Oxoid) plates. Loss of the *pgm* locus was confirmed by colony PCR using primers PGM-F1 and PGM-R2 (see Table S2 in the supplemental material). The resulting strains, KIM6/GFP and KIM6*phoP*Δ/GFP, were made electrocompetent as described previously (13) and were transformed by electroporation with pCD1Ap (24). Transformants were selected on LB agar plates supplemented with 25 μg/ml ampicillin and 10 μg/ml chloramphenicol. The resulting strains were designated KIM5/GFP and KIM5*phoP*Δ/GFP (Table 1).

Bacterial infection of macrophages and analysis of bacterial survival. Mouse macrophage-like cell line J774A.1 was cultured and infected with *Y. pestis* as described previously (25), unless indicated otherwise. For viable count assays macrophages were infected at a multiplicity of infection (MOI) of 5. At different times after infection a viable count assay was performed as described previously (25), except that the sonication step was omitted. For analysis of intracellular survival and replication by fluorescence microscopy, macrophages were grown on coverslips and were infected at an MOI of 5. The conditions used for induction of GFP expression with isopropyl-β-D-thiogalactopyranoside (IPTG), cell fixation with paraformaldehyde, staining of bacteria with anti-*Yersinia* antibody, and fluorescence microscopy have been described previously (25). To analyze expression of GFP under control of the *ugd* promoter, infection with KIM6+/PGFP was carried out as described above, with the following modifications. Macrophages were seeded on polylysine-coated coverslips (BioCoat; Becton Dickinson). Infection was carried out in the absence of gentamicin and IPTG. Before fixation the plate containing the macrophages was centrifuged for 5 min at 200 × *g* to bring bacteria present in the supernatant in contact with the polylysine-coated coverslips.

Phagosome trafficking assays. Infection was carried out at an MOI of 10 with bacteria preinduced for GFP expression as described previously (25). Gentamicin-killed bacteria were prepared by exposing *Y. pestis* cultures preinduced for GFP expression to gentamicin (final concentration, 50 μg/ml) overnight. Viable count assays carried out with samples of the gentamicin-killed bacteria used in these experiments showed that the treatment reproducibly killed >90% of the bacteria. Macrophages were incubated with 1.1-μm latex beads (LB11; Sigma) at a bead/macrophage ratio of 10. Lysosomes were preloaded with ovalbumin conjugated to Texas Red (TROv) (Molecular Probes) by incubating uninfected macrophages for 30 min in complete tissue culture medium containing 50 μg/ml TROv. The cells were then washed twice with phosphate-buffered saline (PBS) and incubated in complete tissue culture medium for 2.5 h to allow TROv to accumulate in lysosomes. Macrophages infected for 5 h were incubated with TROv under the same conditions and then incubated in medium lacking TROv

for 2.5 h to measure the accessibility of *Y. pestis*-containing phagosomes to endocytosed material. All subsequent steps were done at room temperature unless indicated otherwise. Macrophages were fixed and washed as described previously (25). Macrophages exposed to TROv were permeabilized with 0.2% Triton X-100 in PBS for 10 min. For cathepsin D staining, the fixed cells were permeabilized with ice-cold methanol for 30 s. For Lamp1 staining the cells were permeabilized by addition of 0.1% saponin to the blocking solution (PBS containing 3% goat serum). The coverslips were incubated twice for 10 min in blocking solution and then sequentially for 40 min with primary and secondary antibodies diluted in blocking solution. The coverslips were washed three times with PBS and mounted on glass slides in ProLong Gold antifade reagent (Molecular Probes). The coverslips were analyzed by confocal microscopy using a Leica DM IRE2. Images were captured at a magnification of 100× using Leica's LCS software package. The images were analyzed with Adobe Photoshop. Approximately 50 phagosomes or at least three different fields per slide were scored for each infection. Data from three independent experiments were collected, and averages and standard deviations were calculated with Microsoft Excel.

Electron microscopy. Twenty milliliters of a solution containing 10-nm bovine serum albumin (BSA)-gold particles (optical density at 520 nm [OD_{520}], 2; Electron Microscopy Sciences) was placed in dialysis tubing (SpectraPor; molecular weight cutoff, 6,000 to 8,000) and dialyzed in PBS overnight to remove sodium azide. Macrophages were seeded into six-well plates at a density of 1.58×10^5 cells/cm^2 on the day before the experiment and incubated overnight at 37°C in the presence of 5% CO_2. Then 1.5 ml of the dialyzed BSA-gold particle solution supplemented with 10% heat-inactivated fetal bovine serum that had been prewarmed to 37°C was added to each well containing macrophages. After 30 min of incubation at 37°C in the presence of 5% CO_2 to allow pinocytosis of the particles, the BSA-gold particle solution was removed, the macrophages were washed twice with PBS, and incubation was continued for 2.5 h in complete tissue culture medium. Macrophages were infected at an MOI of 20 for 1.5 h as described above. Alternatively, macrophages infected for 5 h were exposed to BSA-gold particles under the same conditions and then incubated for an additional 2.5 h to examine the accessibility of *Y. pestis* phagosomes to newly endocytosed material. Infected macrophages were fixed with 2.5% (vol/vol) glutaraldehyde and 2% (wt/vol) paraformaldehyde in cacodylate buffer (100 mM, pH 7.2 to 7.4) supplemented with 2.5 mM calcium chloride for 30 min. The fixed cells were washed three times with cacodylate buffer for 5 min each time and processed for thin-section transmission electron microscopy by the University Microscopy Imaging Center (SUNY Stony Brook) using a procedure available online (www.umic.sunysb.edu/FIXDEEMB.htm). Images of thin sections were acquired with a JEOL JEM 1200EX transmission electron microscope. Negatives were digitally scanned and subsequently processed using Adobe Photoshop.

RNA isolation. For each microarray data set, three independent RNA isolations were performed (see Table S2 in the supplemental material). KIM10+*phoP*Δ/MMB67EH and KIM10+*phoP*Δ/PhoP (Table 1) cultures were grown in HI broth at 28°C and diluted in HI broth supplemented with 100 μg/ml ampicillin and 500 μM IPTG to obtain an OD_{600} of ∼0.1. Incubation was continued at 28°C with shaking until the cultures reached the logarithmic phase (OD_{600}, ∼0.5 to 0.8). KIM6+ and KIM6+*phoP*Δ cultures were grown overnight in HI broth at 28°C and diluted in HI broth to obtain an OD_{600} of ∼0.1. Incubation was continued at 28°C with shaking until the cultures reached the logarithmic phase (OD_{600}, ∼0.5 to 0.8). Two milliliters of each culture (∼1 × 10^9 to 1.6 × 10^9 cells) was mixed immediately with 4 ml of Bacteria Protect reagent (QIAGEN) and incubated at room temperature for 5 min to stabilize the RNA. The cells were then harvested by centrifugation at 3,800 × *g* for 10 min. The cell pellets were used immediately for RNA isolation or kept at −80°C until they were needed (<2 weeks). The bacterial cells were lysed with 1.5 mg/ml lysozyme (Boehringer Mannheim) in Tris-EDTA for 5 min at room temperature. Total RNA was isolated using a QIAGEN RNeasy mini kit according to the manufacturer's instructions. On-column digestion of genomic DNA was performed using an RNase-free DNase set (QIAGEN). The integrity of the RNA was determined by agarose gel electrophoresis. The RNA concentration and purity were determined using a Nanodrop ND-1000 spectrophotometer.

Generation of fluorescent cDNA probes. Fluorescent cDNA probes were prepared by an indirect aminoallyl labeling method by using protocols obtained from The Institute for Genome Research (TIGR) (http://www.tigr.org/tdb/microarray/protocolsTIGR.shtml), with following changes: 10 μg of total RNA was used for cDNA synthesis, and the reaction mixture contained 300 μM aminoallyl-dUTP and 200 μM dTTP. RNA was degraded after cDNA synthesis using 0.8 μg of RNase A (Boehringer Mannheim) and 1 U of RNase H (Invitrogen) instead of NaOH.

Microarray hybridization and processing. The 70-mer oligonucleotide microarrays representing all ORFs from *Y. pestis* were obtained from TIGR. The microarray slides were prehybridized, washed, and dried immediately before hybridization by using the protocol recommended by TIGR (http://www.tigr.org/tdb/microarray/protocolsTIGR.shtml). For hybridization, cDNA with 150 pmol Cy3 and cDNA with 150 pmol Cy5 were included in a 55-µl hybridization solution containing 25% (vol/vol) formamide, 5× SSC, 0.1% sodium dodecyl sulfate (SDS), and 100 µg/ml of sonicated salmon sperm DNA (1× SSC is 0.15 M NaCl plus 0.015 M sodium citrate). Hybridization was performed under lifter coverslips (25 by 60 mm; Erie Scientific) at 50°C in a humidified chamber for 16 to 20 h. Hybridized arrays were washed with gentle shaking as follows: twice briefly with 2× SSC–0.1% SDS at 50°C, twice for 10 min with 2× SSC–0.1% SDS at 50°C, twice briefly with 0.1× SSC–0.1% SDS at 50°C, twice for 10 min with 0.1× SSC–0.1% SDS, and four times briefly with 0.1× SSC at room temperature. Arrays were dried by placing them into a 50-ml blue cap Falcon tube containing tissue paper in the bottom and were centrifuged at 1,300 × *g* for 2 min at room temperature. Arrays were scanned using an Axon 4000B scanner that was controlled by the GenePix Pro 6 software with a pixel size of 10 µm and two-pass sequential line averaging. The laser power was set to 100%, and PMT gains were subjectively adjusted during prescanning to maximize the effective dynamic range and to limit image saturation. Lossless image files were stored for later analysis.

Statistical analysis of microarray data. A summary of the experimental conditions used to generate the microarray data that were analyzed is shown in Table S2 in the supplemental material. The microarray data were analyzed using the Limma module of the Bioconductor package for the R statistical environment (23, 65). The "normexp" method was used for background correction, followed by print tip loess normalization and between-array normalization of intensities. The microarray data for each gene were fitted to a linear model, and statistics were generated using the lmFit and eBayes functions (65). For experiments involving overexpression of PhoP in KIM10+, duplicate spots for every gene on the slide were used by Limma, while in experiments in which *phoP*+ and *phoP* mutant KIM6+ strains were compared, only the first of the duplicate spots was used by Limma, since Limma cannot currently calculate technical replicates and on-slide replicates in the same analysis. The *P* values displayed were adjusted for multiple testing using the Benjamini and Hochberg method within Limma. Genes with *P* values of <0.05 were considered differentially regulated. Annotations for microarray data were derived from TIGR gal files. "Probe" refers to the gene ID from which the 70-mer probe was designed. "KIM ID" was derived by using the microarray probe sequence in a BLAT (38) search against the KIM CDS sequences from the genome (accession no. NC_004088.1). A single KIM ID could be assigned to multiple probes as the TIGR arrays may contain probes designed for a single gene that is slightly different in CO92 and KIM.

Identification of PhoP-regulated genes by Tn5-lacZ mutagenesis. Plasmid pPhoP2 contains the *phoP* ORF inserted between BamHI and EcoRI sites in pMMB207 (49), placing *phoP* under control of the *tac* promoter in the manner observed previously for pPhoP (25). pPhoP2 was introduced into KIM10+*phoP*Δ to create KIM10+*phoP*Δ/PhoP2 (Table 1). *E. coli* SM10λ*pir* carrying plasmid pAJD273 (provided by Virginia Miller) was used as the transposon donor. The pAJD273 plasmid contains the Tn5 transposase and a mini-Tn5 element with a promoterless *lacZYA* operon and the selective marker for spectinomycin and streptomycin resistance flanked by Tn5 inverted repeats. KIM10+*phoP*Δ/PhoP2 was mated with SM10λ*pir*/pAJD273, and *Y. pestis* colonies containing transposon insertions were selected on LB agar plates containing spectinomycin, streptomycin, and chloramphenicol. Colonies were patched onto master plates having the same composition and then replica plated onto LB agar plates containing either 5-bromo-4-chloro-3-indolyl-β-D-galactopyranoside (X-Gal) (40 µg/ml) or X-Gal and IPTG (100 µM) in addition to the antibiotics. Colonies that were darker blue on plates with IPTG than on plates without IPTG were picked from the master plate and tested by using the β-galactosidase assay. Overnight cultures of each strain were diluted in fresh HI broth with or without 500 µM IPTG and incubated for 3 h at 28°C with shaking. The OD_{600} of each culture was determined, and 0.5 ml of culture was mixed with 0.5 ml of Z buffer (46). Bacterial cells were lysed by adding 55 µl of 0.1% SDS and 55 µl of chloroform. Two hundred microliters of *o*-nitrophenyl-β-D-galactopyranoside (4 mg/ml) was added to each lysate, and the reaction mixtures were incubated at room temperature. Reactions were stopped by adding 0.5 ml of 1 M Na_2CO_3. The OD_{420} and OD_{550} of each sample were determined and used to calculate the number of Miller units (46). Measurement was performed in triplicate. Mutants with PhoP-regulated *lacZ* insertions were tested in macrophage survival and replication assays using microscopy in combination with fluorescent antibodies as described above. To allow PhoP expression throughout the experiment, the HI broth used for the overnight cultures and the tissue culture medium used for infection were supplemented with 100 µM IPTG.

Sequence analysis of Tn5-lacZ insertion mutants. Genomic DNA was isolated from 10 ml of a culture grown overnight at 28°C in HI broth using the QIAGEN Genomic Tip-100 genomic DNA protocol. The isolated DNA was dissolved in QIAGEN EB buffer and sheared by adding glass beads and vortexing the mixture for 3 to 5 min. Five micrograms of genomic DNA was used for cycle sequencing in a 40-µl reaction mixture containing 16 µl of Big Dye terminator mixture (Applied Biosystems) and 25 pmol of sequencing primer (either TN5SEQ1 or TN5SEQ2). Cycle sequencing was performed with an Eppendorf MasterCycler using the following conditions: 95°C for 5 min, followed by 100 cycles of 30 s at 95°C, 58°C for 20 s, and 65°C for 4 min.

Statistical analysis. A statistical analysis of the phagosome trafficking data was performed using repeated-measures analysis of variance and the Tukey posttest (Graphpad InStat). *P* values of <0.05 were considered significant.

Microarray data accession number. The accession number for the microarray data is E-MEXP-712 and E-MEXP-713.

RESULTS

Nascent phagosomes containing *phoP*+ or *phoP* mutant *Y. pestis* undergo fusion with lysosomes. To study the role of PhoP in the survival of *Y. pestis* and trafficking of its phagosomes in macrophages, strains KIM5/GFP and KIM5*phoP*Δ/GFP (Table 1) were used to infect J774A.1 cells. J774A.1 cells have been widely used as model macrophages to study survival and trafficking of intracellular bacteria (6, 10, 47). Prior to infection the bacteria were grown at 28°C to repress Yop and F1 expression. After infection the macrophages were incubated in the presence of gentamicin to kill extracellular bacteria. The survival of intracellular bacteria was measured by a viable count assay. As expected based on previous results (25, 54), KIM5*phoP*Δ/GFP was defective for survival in J774A.1 macrophages, as shown by the reduction in the number of viable bacteria that could be recovered from macrophages over the course of an 8-h infection (Fig. 1A). In contrast, no decrease in the number of viable bacteria was observed for *phoP*+ KIM5/GFP during the first 8 h postinfection (Fig. 1A). KIM5/GFP was able to replicate in these macrophages between 8 and 24 h after infection, as shown by fluorescence microscopy following induction of GFP expression (Fig. 1B to D).

Phagosome trafficking assays were carried out to determine if vacuoles containing *phoP*+ or *phoP* mutant *Y. pestis* interact differently with the lysosomal compartment. Initially, electron microscopy was used to detect fusion between *Y. pestis*-containing vacuoles and lysosomes containing BSA-gold particles. J774A.1 macrophages were allowed to pinocytose BSA-gold and then incubated to allow the particles to accumulate in lysosomes. The macrophages were then infected with KIM5/GFP or KIM5*phoP*Δ/GFP, and at 1.5 h postinfection samples were fixed and processed for electron microscopy. Figure 2 shows representative images of phagosomes containing either *phoP*+ bacteria (Fig. 2A) or *phoP* mutant bacteria (Fig. 2B). The majority of phagosomes containing either *phoP*+ or *phoP* mutant *Y. pestis* contained gold particles and therefore had fused with lysosomes. In two independent experiments only 2 of 48 phagosomes and 4 of 30 phagosomes containing *phoP*+ *Y. pestis* did not contain observable gold particles.

We next used confocal microscopy to quantify interactions between *Y. pestis*-containing phagosomes and lysosomes. GFP expression was induced prior to infection to allow detection of bacteria. Macrophages were allowed to pinocytose TROv in order to label lysosomes, as was done for BSA-gold particles. Alternatively, antibodies specific for cathepsin D or Lamp1,
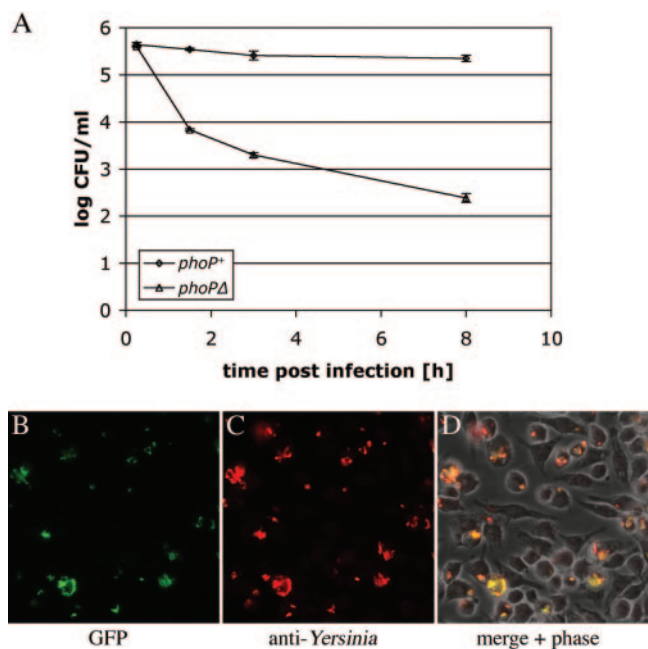
FIG. 1. Survival of *phoP+* and *phoP* mutant *Y. pestis* strains in macrophages as determined by CFU assay or fluorescence microscopy. J774A.1 cells were infected with KIM5/GFP or KIM5*phoP*Δ/GFP at an MOI of 5 and then incubated in the presence of gentamicin as described in Materials and Methods. (A) The infected cells were lysed at different times, and serial dilutions of the lysates were plated to determine the number of intracellular bacteria by a CFU assay. The data are the results of one representative experiment, and values from triplicate wells were averaged. The error bars indicate standard deviations. (B to D) Macrophages were infected with KIM5/GFP for 23 h, exposed to 500 μM IPTG for 1 h to induce GFP expression, and then fixed and stained with an anti-*Yersinia* antibody and a secondary antibody conjugated to Alexa-594. Fluorescence or phase-contrast microscopy images at a magnification of ×40 were captured using a digital camera. (B and C) Representative images of GFP fluorescence and Alexa-594 fluorescence (anti-*Yersinia*), respectively. (D) Fluorescence images merged with a phase-contrast image.

two proteins that are found in late endosomes or lysosomes, were used to label these compartments in infected macrophages. In parallel, some macrophages were allowed to phagocytose 1.1-μm latex beads, and the trafficking of phagosomes containing these particles was compared to the trafficking of phagosomes containing bacteria. After 1.5 h of infection, the cells were fixed, and colocalization of a fluorescent signal with phagosomes was determined by confocal microscopy. Figure 3 shows representative results for macrophages infected with KIM5/GFP, and Fig. 4A shows a summary of the results for all conditions. Approximately 75% to 90% of the phagosomes containing KIM5/GFP, KIM5*phoP*Δ/GFP, or beads contained the TROv label at 1.5 h postinfection (Fig. 4A), which indicated that the majority of phagosomes containing either *phoP+* or *phoP* mutant *Y. pestis* had fused with lysosomes during the first 1.5 h of infection. Approximately 70% to 80% of the phagosomes containing beads or *Y. pestis* exhibited staining for Lamp1 at 1.5 h (Fig. 4A), which also indicated that the nascent vesicles fused with lysosomes or late endosomes. Cathepsin D colocalized to lesser extents with phagosomes containing beads (50%), KIM5*phoP*Δ/GFP (40%), or KIM5/GFP (30%) at 1.5 h (Fig. 4A). These results could reflect reduced delivery of cathepsin D into phagosomes or a reduced ability to detect this marker compared to the ability to detect Lamp1 or TROv.

Vacuoles containing viable *phoP+ Y. pestis* enlarge to form spacious phagosomes and remain accessible to the endocytic pathway for up to 8 h postinfection. To determine if vacuoles containing *Y. pestis* remain accessible to the lysosomal compartment at a later time, the presence of lysosomal markers in 8-h phagosomes was also examined. It was not possible to analyze phagosomes containing *phoP* mutant bacteria at 8 h postinfection since few intact bacteria were present in macrophages at this time (data not shown) (25). Instead, some macrophages were incubated with gentamicin-killed KIM5/GFP, because we found that gentamicin-killed *phoP+ Y. pestis* cells do remain intact in phagosomes for up to 8 h postinfection
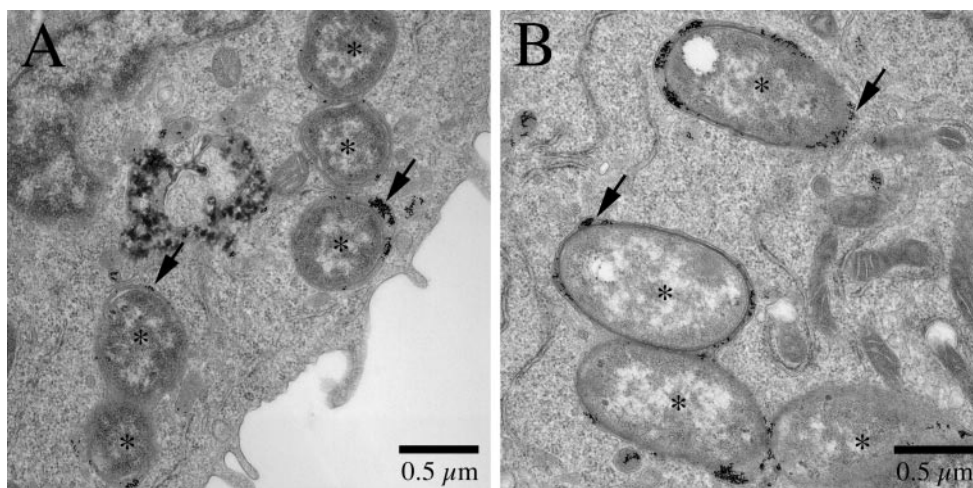

FIG. 2. Analysis of phagosome-lysosome fusion at 1.5 h postinfection by thin-section electron microscopy. J774A.1 cells were allowed to pinocytose 10-nm BSA-gold particles for 30 min. After 2.5 h of incubation to allow the gold particles to traffic through the endosomal pathway and to accumulate in lysosomes, the macrophages were infected with *phoP+* or *phoP* mutant *Y. pestis* (MOI, 20) for 1.5 h. The infected macrophages were fixed and prepared for thin-section electron microscopy as described in Materials and Methods. (A) Phagosomes containing KIM5/GFP. (B) Phagosomes containing KIM5*phoP*Δ/GFP. Bacteria are indicated by asterisks. The arrows indicate gold particles in phagosomes.

anti-Lamp1   GFP   merge + DIC

anti-Cathepsin D   GFP   merge + DIC
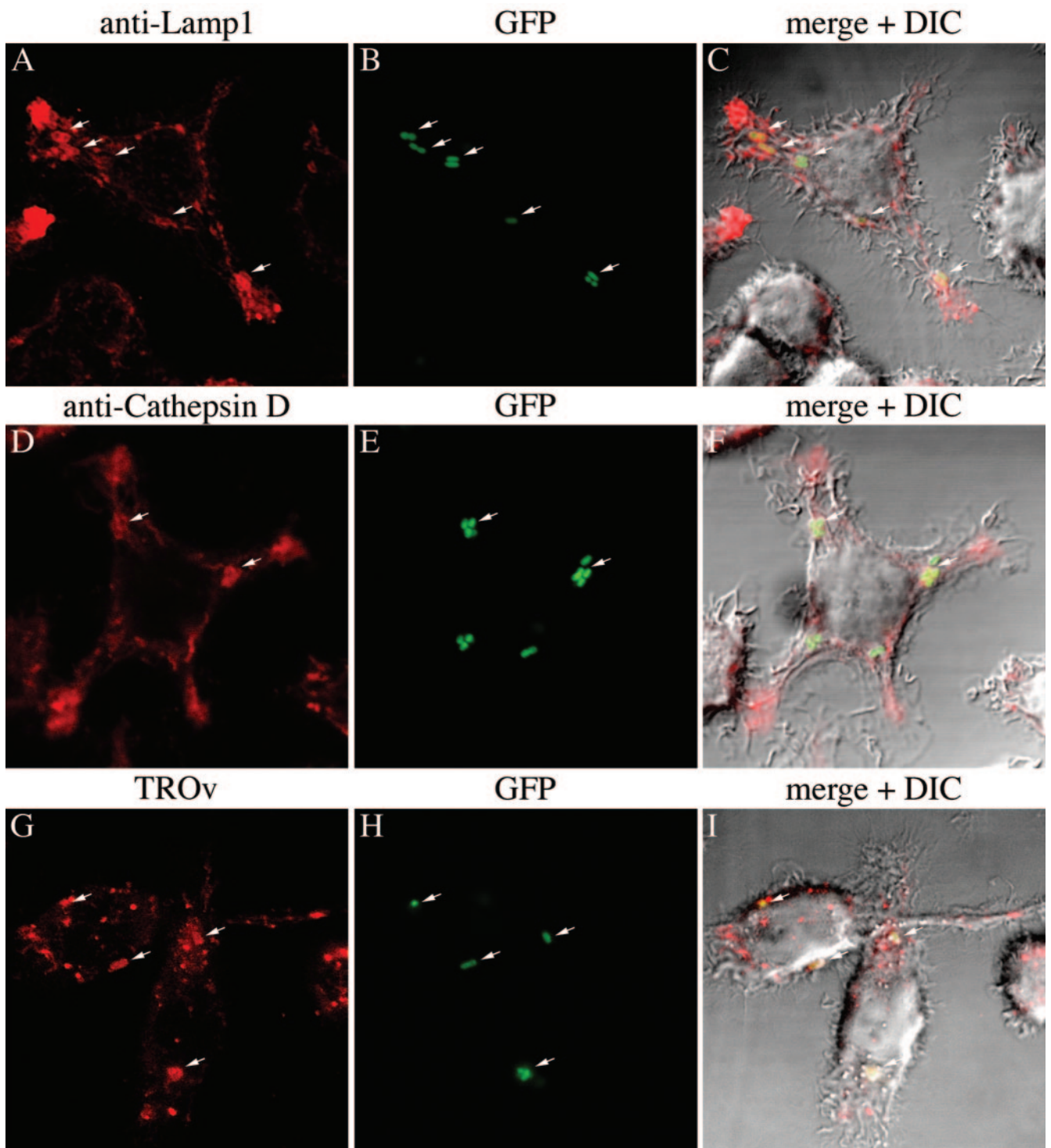
TROv   GFP   merge + DIC

FIG. 3. Colocalization of *Y. pestis*-containing phagosomes with different lysosomal markers as determined by confocal microscopy. J774A.1 cells were infected with GFP-expressing *Y. pestis* strain KIM5/GFP (MOI, 10) for 1.5 h. The infected macrophages were fixed and incubated with antibodies against the lysosomal membrane protein Lamp1 (A to C) or the lysosomal protease cathepsin D (D to F). Binding of the primary antibodies was detected by incubation with secondary antibody conjugated to Alexa-647 (Lamp1) or Alexa-633 (cathepsin D). Alternatively, macrophages were allowed to pinocytose the fluid phase tracer TROv for 30 min and then incubated for 2.5 h to allow TROv to accumulate in lysosomes prior to infection (G to I). Macrophages were analyzed by fluorescence confocal or differential interference contrast (DIC) microscopy. (A and D) Alexa fluorescence signals. (G) Texas Red fluorescence signal. (B, E, and H) GFP signals. (C, F, and I) Merged fluorescence and differential interference contrast images.
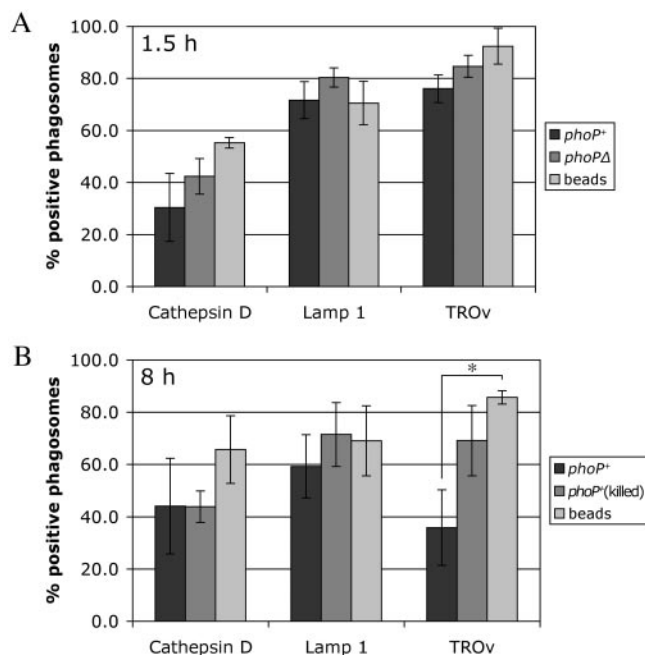
FIG. 4. Percentages of *Y. pestis*- and bead-containing phagosomes associated with a lysosomal marker. (A) J774A.1 macrophages were infected with GFP-expressing *Y. pestis* strain KIM5/GFP or KIM5 *phoP*Δ/GFP (MOI, 10) or incubated with latex beads. After 1.5 h of incubation, the macrophages were fixed and processed as described in the legend to Fig. 3 to detect colocalization of phagosomes with Lamp1, cathepsin D, or TROv by confocal microscopy. For the TROv experiments, macrophages were allowed to pinocytose the label for 30 min and then incubated in the absence of TROv for 2.5 h prior to incubation with bacteria or beads. (B) J774A.1 macrophages were infected with GFP-expressing live or gentamicin-killed *Y. pestis* KIM5/GFP or incubated with latex beads. After 8 h of incubation, the macrophages were fixed and processed as described above for confocal microscopy. For the TROv experiments, the label was added 5 h after exposure to bacteria or beads for 30 min. Incubation was then continued in the absence of TROv for 2.5 h to allow the label to accumulate in lysosomes. For each experiment and each marker 50 phagosomes were analyzed by confocal microscopy to determine the colocalization of the GFP signal with the lysosomal marker. The data are the averages of three independent experiments. The error bars indicate standard deviations. The asterisk indicates that the difference is statistically significant.

(data not shown). The results of experiments using cathepsin D and Lamp1 antibodies indicated that the extent to which phagosomes containing viable *phoP*[+] *Y. pestis* retained these lysosomal markers was similar to the extent to which vacuoles containing dead bacteria or beads retained the markers (Fig. 4B). For experiments using TROv, macrophages were allowed to pinocytose the label 5 h after they had internalized bacteria or latex beads. The macrophages were then washed and incubated for an additional 2.5 h to allow TROv to traffic through the endocytic pathway. The cells were then fixed and prepared for observation by confocal microscopy. At 8 h postinfection 85% of the latex bead phagosomes colocalized with TROv, and approximately 70% of the phagosomes containing killed KIM5/GFP contained the TROv label (Fig. 4B). Unexpectedly, only 35% of the phagosomes containing viable KIM5/GFP contained detectable levels of TROv at 8 h postinfection (Fig. 4B), suggesting that although 8-h vacuoles containing live

Y. pestis retained markers of lysosomes (cathepsin D and Lamp1), they were less accessible to the endocytic pathway than vacuoles containing beads or killed bacteria were.

Electron microscopy and BSA-gold labeling were used to investigate further the accessibility of phagosomes containing viable *Y. pestis* to the lysosomal compartment. Macrophages infected with viable KIM5/GFP were allowed to pinocytose BSA-gold particles at 5 h postinfection, and at 8 h postinfection the cells were fixed and prepared for electron microscopy. The majority (>90%) of phagosomes detected contained gold particles, suggesting that fusion with lysosomes or other vesicles of the endocytic pathway had occurred (Fig. 5). However, two types of phagosomes were observed. The phagosomal membrane was tightly associated with the bacteria in 50% of the vacuoles (Fig. 5A). The other 50% of the phagosomes were spacious, with a large space separating the bacteria from the phagosomal membrane (Fig. 5B). In preliminary experiments, no spacious vacuoles were observed in macrophages that internalized killed KIM5/GFP (data not shown). The difference between colocalization of TROv with phagosomes containing viable bacteria and colocalization of TROv with phagosomes containing beads or killed bacteria (Fig. 4B) could therefore have been due to dilution of TROv in a spacious phagosome, causing the strength of the signal to fall below the limit detectable by confocal microscopy. Taken together, the results of these trafficking assays suggest that *Y. pestis* survives and replicates in a macrophage vacuole that initially fuses with lysosomes and then enlarges into a spacious compartment while remaining accessible to the endocytic pathway for up to 8 h postinfection. A *Y. pestis phoP* mutant may be rapidly killed in a macrophage because the bacteria are not able to adapt to the potentially hostile environment of the vacuole.

Identification of PhoP-regulated genes important for survival of *Y. pestis* in phagosomes. PhoP can faithfully activate its target genes in a PhoQ-independent manner when it is overexpressed in *S. enterica* serovar Typhimurium, apparently due to self-association of PhoP at high concentrations (42). We took advantage of this property to identify PhoP-regulated genes that are important for survival of *Y. pestis* in the macrophage phagosome. *Y. pestis* strain KIM10+*phoP*Δ/PhoP2 was subjected to mutagenesis using a Tn5-*lacZ* transposon. This strain has an in-frame deletion in *phoP* and carries a wild-type copy of *phoP* under control of the IPTG-inducible *tac* promoter on a plasmid (Table 1). Colonies of *Y. pestis* Tn5-*lacZ* insertion mutants were screened for a LacZ[+] phenotype when they were grown on IPTG-containing medium and for a LacZ[−] phenotype when they were grown in the absence of IPTG.

Among the 10,000 insertion mutants that were screened we identified 22 insertion mutants that had a PhoP-dependent LacZ[+] phenotype. Each mutant was tested to determine its ability to survive and replicate in macrophages, and genomic sequencing was carried out to determine the site of transposon insertion. The transposon insertion site of one mutant with a wild-type survival phenotype could not be determined, while the approximate transposon insertion sites for all other mutants could be determined; the results are summarized in Table 2. Several mutants had insertions that were distant from an annotated ORF (e.g., mutant 110-13) or were in an inverted orientation relative to a predicted ORF (e.g., mutants 73-73 and 51-62). These mutants had wild-type survival phenotypes and thus
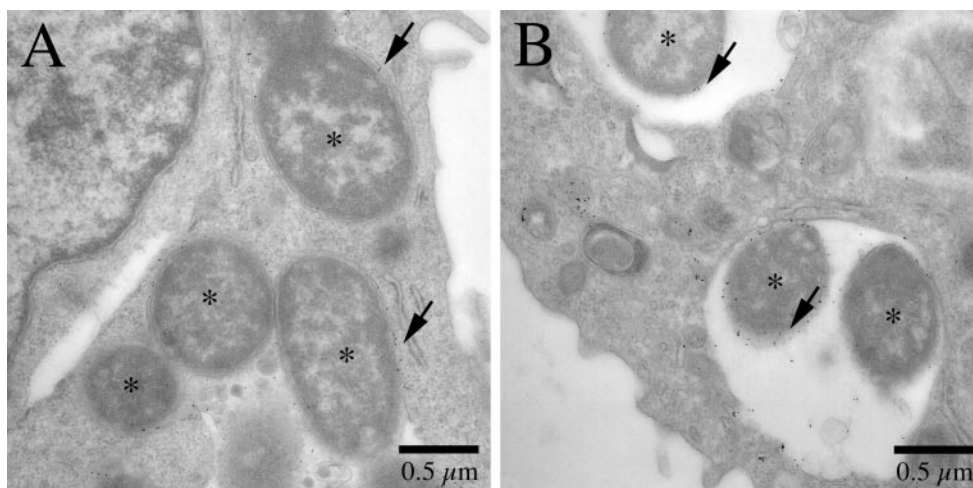
FIG. 5. Analysis of phagosome-lysosome fusion at 8 h postinfection by thin-section electron microscopy. J774A.1 macrophages were infected with *Y. pestis* KIM5/GFP at an MOI of 20. After 5 h of infection, the macrophages were allowed to pinocytose 10-nm BSA-gold particles for 30 min. After incubation for an additional 2.5 h, the infected macrophages were fixed and processed for thin-section electron microscopy. (A) Tight phagosomes containing KIM5/GFP. (B) Spacious phagosomes containing KIM5/GFP. Bacteria are indicated by asterisks. The arrows indicate gold particles in phagosomes.

were not studied further. Other mutants contained insertions in or near ORFs homologous to PhoP-regulated genes in *S. enterica* serovar Typhimurium (Table 2). Insertions in three of these ORFs, ORFs y1820, y1921, and y2147, resulted in a defective intracellular survival phenotype (Table 2). ORF y1820 is homologous to *mgtC* in *S. enterica* serovar Typhi-

murium (7). In *S. enterica* serovar Typhimurium *mgtC* is co-transcribed in a two-gene operon with *mgtB*, which encodes an Mg^{2+} transporter (34). There is a similar genetic arrangement in *Y. pestis*, since an *mgtB*-like gene (y1821) is downstream of y1820 (7). *S. enterica* serovar Typhimurium *mgtC* mutants are defective for growth in Mg^{2+}-limited medium and in macro-

TABLE 2. Summary of PhoP-regulated Tn5-*lacZ* insertion mutants

Mutant	Insertion site[a]	Survival in macrophages[c]	Annotation[e]
28-16	Unknown	+	Not applicable
25-36	5′ to y0020	+	YPO3722, methionine synthase
91-8	y0020		
73-73	y0455[b]	+	Hypothetical protein
20-17	y0513	+	YPO0256, two-component sensor, *spiR*/*ssrA*
32-70	y0513		
74-14	y0513		
110-13	3′ to y0564	+	YPO0304, hypothetical protein
51-62	y0943[b]	+	YPO3247, putative adhesin
88-65	3′ to y1820	Defective[d]	YPO1660, Mg^{2+} transport ATPase protein C, *mgtC*
62-41	y1921	Defective	YPO2418, mannosyltransferase family protein, *pmrK*/*pqaB*
93-11	y1921		
105-55	y1921		
37-48	y2124	+[d]	YPO2292, putative lipoprotein
95-70	3′ to 2124		
21-29	y2147	Defective	YPO2174, nucleotide sugar dehydrogenase, *ugd*
98-31	y2147		
100-53	3′ to y2563	+[d]	YPO1744, hypothetical protein, *pagP*
61-22	y2608	+	YPO1559, hypothetical protein
31-05	y2816	+[d]	YPO1363, putative virulence factor, *somA*
75-11	y2816		
41-48	y3948	+	YPO0164, putative membrane receptor protein

[a] Tranposon insertion sites are indicated by using locus tag nomenclature for ORFs from the KIM genomic sequence (accession no. NC_004088) (15).
[b] Reading frames of *lacZ* and ORF are in inverse orientation.
[c] The survival of bacteria carrying insertions in the genes was tested in J774A.1 cells using anti-*Yersinia* staining and immunofluorescence microscopy as described in Materials and Methods. A plus sign indicates that the survival phenotype was indistinguishable from that of the parental strain; defective indicates that survival was substantially reduced.
[d] The macrophage survival phenotype was confirmed by insertion of the *kan* cassette into the corresponding ORF.
[e] The annotation is for the CO92 genome (accession no. NC_003143) (55), and the locus tag nomenclature for CO92 is shown; the annotation for mutant 73-73 (y0455) is the annotation for the KIM genome.

TABLE 3. Selected genes determined by microarray to be positively regulated under *phoP* overexpression conditions[a]

KIM ID[b]	Probe[c]	Annotation[d]	*P* value	Fold change
y1794	YPO1634	Response regulator protein (*phoP*)	1.81E-05	25.9
y1918	YPO2421	Probable glycosyl transferase (*pmrF*)	6.22E-06	13.1
y1917	YPO2422	Conserved hypothetical protein (*pmrH*)	3.07E-05	13.0
y1919	YPO2420	Probable formyl transferase (*pmrI*)	3.44E-06	11.0
y2124[e]	YPO2292	Putative lipoprotein	1.31E-05	10.4
y1920	YPO2419	Conserved hypothetical protein (*pmrJ*)	3.44E-06	9.6
y1877	YPO1715	Probable *N*-acetylmuramoyl-L-alanine amidase	6.22E-06	9.5
y2147[e]	YPO2174	Putative nucleotide sugar dehydrogenase (*ugd*)	1.31E-05	9.0
y2816[e]	YPO1363	Putative virulence factor (*somA*)	6.40E-05	8.5
y1921[e]	YPO2418	Mannosyltransferase family protein (*pmrK*)	6.40E-05	7.7
y1795	YPO1635	Putative lipoprotein	1.31E-05	7.2
	YPO1659	Hypothetical protein	2.38E-04	6.9
y1922	YPO2417	Putative membrane protein (*pmrL*)	6.22E-06	6.7
y2608[e]	YPO1559	Hypothetical protein	3.06E-05	6.4
y0838	y0838	Putative dehydrogenase	9.93E-06	5.2
y1923	YPO2416	Putative membrane protein (*pmrM*)	1.05E-05	5.0
y0838	YPO3352	Putative zinc-binding dehydrogenase	4.04E-04	4.4
y3284	y3284	Hypothetical protein	4.94E-04	3.9
y0839	YPO3351	Putative dehydrogenase	8.24E-04	3.7
y1741	YPO2449	Putative LuxR family regulatory protein	5.77E-04	3.2
y0447	y0447	Hypothetical protein	8.22E-05	3.2
y0840	y0840	Putative dihydroxyacetone kinase	1.74E-02	3.1
y0840	YPO3350	Putative dihydroxyacetone kinase	5.33E-04	3.1
y0245	YPO3624	Putative aliphatic sulfonate binding protein	2.30E-03	2.9
y3948[e]	YPO0164	Putative membrane receptor protein	1.55E-02	2.8
y0243	YPO3626	Putative aliphatic sulfonate transport permease protein	1.22E-03	2.7
y0246	YPO3623	Putative NAD(P)H-dependent flavin mononucleotide reductase	5.77E-04	2.7
y0244	YPO3625	Alkanesulfonate monooxygenase	6.16E-04	2.6
y3966	YPO0185	Putative taurine dioxygenase	7.35E-03	2.6
y2866	YPO1318	Putative ABC transport ATP-binding subunit	2.98E-02	2.5
y3964	YPO0183	Putative taurine transport ATP-binding protein	2.50E-04	2.4
y3968	YPO0187	Putative glycosyl transferase	1.86E-02	2.4
y0447	YPO3783	Putative membrane protein	2.68E-04	2.4
y2076	YPO2234	Putative carbon starvation protein A	1.70E-02	2.3
	YPO1366	Cold shock-like protein	8.36E-03	2.3
y0025	YPO3717	Putative membrane protein	8.09E-03	2.3
y1803	YPO1642	Sucrose operon repressor LacI family	3.79E-03	2.3
y1189	YPO2615	Putative amino acid-binding protein precursor	8.36E-03	2.2
y3965	YPO0184	Putative taurine transport system permease protein	6.97E-03	2.2
y2865	YPO1319	Putative ABC transport integral membrane subunit	1.19E-02	2.2

[a] The 40 genes with greatest positive changes are shown.
[b] Locus tag for the KIM sequence, if applicable.
[c] Locus tag for CO92 or KIM corresponding to the oligonucleotide.
[d] Annotation for the CO92 sequence. Selected gene designations are indicated in parentheses.
[e] Gene identified as PhoP regulated in the Tn*5-lacZ* screen.

phages. Since the phenotype of an *S. enterica* serovar Typhimurium *mgtC* mutant could be rescued by exposing infected macrophages to excess Mg^{2+}, it has been suggested that the phagosome is an Mg^{2+}-limited environment and that *mgtC* plays a role in Mg^{2+} uptake (6). ORFs y1921 and y2147 are homologous to *pmrK* and *ugd* of *S. enterica* serovar Typhimurium, respectively, which are required for modification of lipopolysaccharide with aminoarabinose (19, 26). The *pmrK* gene is the fifth gene in the seven-gene *pmr* operon; the products of this locus comprise a pathway for the biosynthesis of 4-aminoarabinose and its addition to lipid A (27, 28). The genetic structure of the *pmr* operon in *Y. pestis* is similar to that in *S. enterica* serovar Typhimurium (44). The product of *pmrK* is a lipid transferase that acts in the last step of the pathway by adding 4-aminoarabinose to lipid A. The *ugd* gene is not linked to the *pmr* operon, but its product, a UDP-glucose dehydrogenase, catalyzes the formation of UDP-glucoronic acid, a precursor of 4-aminoarabinose. Addition of 4-aminoarabinose

to lipid A results in a positively charged lipid A molecule. Bacteria that are able to modify their outer membrane in this way have been shown to be more resistant to antimicrobial peptides, such as polymyxin B (27, 50, 61). Insertions in other ORFs homologous to PhoP-regulated genes in *S. enterica* serovar Typhimurium did not result in defective intracellular survival phenotypes. Mutants 20-17, 32-70, and 74-14 had insertions in ORF y0513, which is a homolog of the *S. enterica* serovar Typhimurium *spiR* (*ssrA*) gene. The *spiR* gene encodes a sensor kinase that regulates expression of TTSS genes in *Salmonella* pathogenicity island 2 (SPI-2) (31, 51). Other ORFs identified in this screen that are homologous to *S. enterica* serovar Typhimurium PhoP-regulated genes but are dispensable for intramacrophage survival of *Y. pestis* are y2563 (*pagP*) and y2816 (*somA*). Both *pagP* and *somA* are important for resistance of *S. enterica* serovar Typhimurium to antimicrobial peptides (16, 19, 26). Finally, several ORFs identified in this screen encode hypothetical proteins (e.g., y0020, y2124,
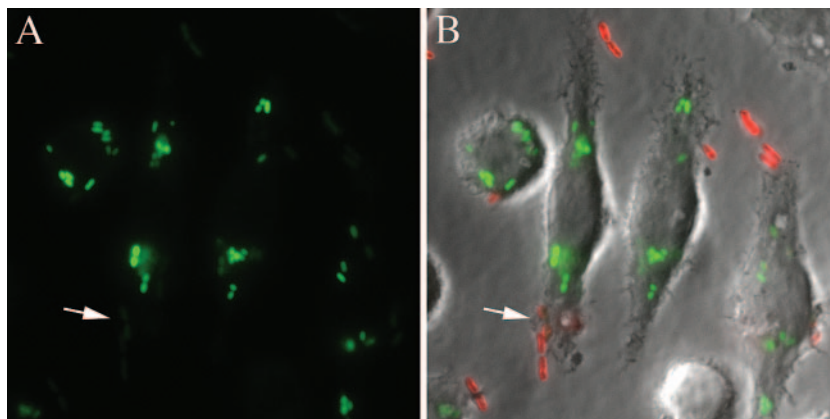
FIG. 6. Analysis of *ugd* promoter activation in intracellular *Y. pestis* by fluorescence microscopy. J774A.1 macrophages were infected (MOI, 5) with *Y. pestis* KIM6+/PGFP, which expresses GFP under control of the *ugd* promoter. The macrophages and bacteria were incubated together in tissue culture medium for 3.5 h in the absence of gentamicin. After fixation, extracellular bacteria were stained with anti-*Yersinia* antibody and a secondary antibody conjugated to Alexa-594. Fluorescence and phase-contrast microscopy images at a magnification of ×100 were captured using a digital camera. (A) GFP fluorescence. (B) GFP and Alexa-594 fluorescence images merged with a phase-contrast image. The arrow indicates extracellular bacteria that are in the process of being phagocytosed.

y2608, and y3948), but none of these ORFs appear to be necessary for survival of *Y. pestis* in macrophages (Table 2).

To confirm and extend the results of the genetic screen, oligonucleotide microarrays were used to identify *Y. pestis* genes that are differentially regulated under *phoP* overexpression conditions. RNA was isolated from cultures of two isogenic *Y. pestis* strains, one overexpressing *phoP* (KIM10+*phoP*Δ/PhoP) and the other not expressing *phoP* (KIM10+*phoP*Δ/MMB67EH) (Table 1). Cy5- and Cy3-labeled cDNAs prepared from the RNA samples were hybridized to oligonucleotide microarrays representing 4,829 *Y. pestis* ORFs. A total of 188 genes were significantly ($P < 0.05$) differentially regulated in the two strains (see Table S3 in the supplemental material). Table 3 shows the 40 genes with the greatest changes that were positively regulated by PhoP overexpression. The first gene is *phoP*, and the data confirmed that it was highly overexpressed under the conditions used. Six genes identified in the Tn*5-lacZ* screen were identified as PhoP-regulated genes in the microarray analysis (Table 3). Interestingly, five of these genes (y2124, y2147, y2816, y1921, and y2608) were among the most differentially expressed genes under PhoP overexpression conditions, with changes of 6.4-fold or greater (Table 3). Seven genes identified in the Tn*5-lacZ* screen were not identified as PhoP-regulated genes in the microarray analysis performed with PhoP-overexpressing bacteria. Two of these genes are y1820 and y2563, which are homologous to PhoP-regulated genes in *S. enterica* serovar Typhimurium (*mgtC* and *pagP*, respectively). Other PhoP-regulated genes identified in the microarray analysis that are interesting candidates for intracellular survival functions include genes encoding a putative ABC transporter system (y2865 and y2866) (Table 3).

Expression of *ugd* is upregulated inside macrophages. It is thought that PhoP in *S. enterica* serovar Typhimurium is activated in response to antibacterial peptides, a low pH, a low Mg^{2+} concentration, and other signals encountered in macrophage phagosomes (2, 26, 53). Recently, Winfield et al. demonstrated that PhoP binds directly to the promoter of y2147 (referred to here as *ugd*) and activates transcription of this gene under low-Mg^{2+} conditions in vitro (72). To determine whether PhoP activates gene expression when *Y. pestis* is in macrophage phagosomes, a plasmid encoding GFP under control of the *ugd* promoter was constructed. *Y. pestis* harboring this plasmid (KIM6+/PGFP) (Table 1) was used to infect macrophages in the absence of gentamicin. At different times after infection, the cells were fixed and observed by phase-contrast and fluorescence microscopy. At the beginning of the infection the bacteria in the inoculum exhibited low but detectable levels of green fluorescence. After 3.5 h of infection, intracellular bacteria showed increased green fluorescence, while extracellular bacteria showed only background levels of fluorescence (Fig. 6). The results of this experiment indicate that PhoP activates expression of *ugd* within several hours after *Y. pestis* is internalized in a macrophage phagosome.

***Y. pestis ugd* and *mgtC* mutants are defective for early survival in macrophage phagosomes.** The Tn*5-lacZ* mutagenesis screen identified *ugd*, y1921 (designated *pmrK*), and y1820 (designated *mgtC*) as genes that are important for survival of *Y. pestis* in macrophages (Table 2). Based on homology with genes in *S. enterica* serovar Typhimurium, the products of *ugd* and *pmrK* are predicted to increase bacterial resistance to antimicrobial peptides present in phagosomes, while the product of *mgtC* is hypothesized to promote acquisition of Mg^{2+} in an Mg^{2+}-limited environment in the phagosome (26). To further investigate the importance of these genes for survival of *Y. pestis* in macrophage phagosomes, *ugd*Δ and *mgtC*::*kan* mutants were constructed (Table 1) and compared with the parent (KIM6+) in terms of survival in macrophages using a viable count assay performed at different times after infection. The *ugd*Δ and *mgtC*::*kan* mutants exhibited decreased intracellular survival between 5 and 8 h postinfection compared to the survival of KIM6+ (Fig. 7). The *ugd*Δ mutant appeared to be more defective for intracellular survival than the *mgtC*::*kan* mutant at early times (Fig. 7). Interestingly, despite the survival defect observed at early infection times, the number of *ugd* mutant cells increased between 8 h and 24 h postinfection (Fig. 7). The number of *mgtC* mutant cells did not increase
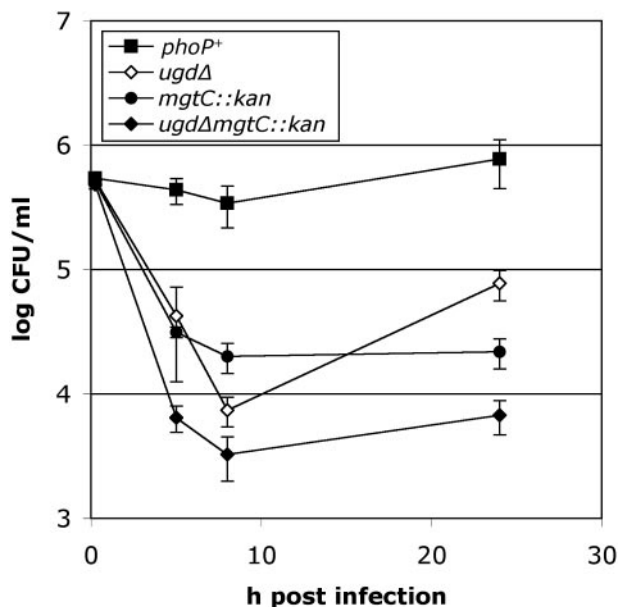
FIG. 7. Survival of *ugd*, *mgtC*, and *ugd mgtC* mutant *Y. pestis* strains in macrophages as determined by a viable count assay. J774A.1 macrophages were infected (MOI, 5) with KIM6+, KIM6+*ugd*Δ, KIM6+ *mgtC*::*kan*, or KIM6+*ugd*Δ*mgtC*::*kan* mutant bacteria. The infected macrophages were incubated in the presence of gentamicin, and at different times the numbers of intracellular bacteria were determined by a viable count assay. The data are averages of three experiments performed with triplicate wells, and the error bars indicate standard deviations.

between 8 h and 24 h postinfection (Fig. 7). Experiments utilizing fluorescence microscopy in combination with induction of GFP expression confirmed that the number of *ugd* mutant cells in macrophages increased between 8 and 24 h postinfection, while the number of *mgtC* mutant cells did not increase (data not shown). These results indicated that although *ugd* and *mgtC* are important for early survival in the macrophage phagosome, bacteria defective for these genes that escape killing within the first 8 h of infection are able to survive (*mgtC*) and replicate (*ugd*) after 8 h. A *ugd*Δ *mgtC*::*kan* double mutant of KIM6+ was constructed, and its ability to survive in macrophages was compared with the abilities of the *mgtC*::*kan* and *ugd*Δ single mutants and the parental strain to survive. Figure 7 shows that the ability of the *ugd*Δ *mgtC*::*kan* double mutant to survive in macrophages was more severely impaired than the ability of either of the single mutants to survive in macrophages. These results indicate that the products of *mgtC* and *ugd* act in distinct pathways to enable *Y. pestis* to survive in macrophages.

DISCUSSION

The aims of this study were to better characterize the vacuole in macrophages which contains *Y. pestis* and to identify genes required for survival in this compartment. Based on our results we concluded that the majority of *Y. pestis*-containing phagosomes fuse with lysosomes and remain accessible to endocytic traffic for up to 8 h postinfection and that PhoP-regulated genes involved in lipopolysaccharide modification and

adaptation to Mg^{2+} limitation are required for bacterial survival in this hostile vacuole.

Two previous studies examined interactions between lysosomes and phagosomes in macrophages infected with *Y. pestis*. Straley and Harmon preloaded lysosomes of peritoneal macrophages with thorium dioxide and, using electron microscopy, obtained evidence that there was fusion between lysosomes and phagosomes containing *Y. pestis* at 1 h postinfection (67). The percentage of phagosomes that fused with lysosomes was not determined in this study (67). Charnetzky and Shuford labeled lysosomes of peritoneal macrophages with acridine orange and, using fluorescence microscopy, found that ~80% of phagosomes containing *Y. pestis* had fused with lysosomes at 2.5 h postinfection (12). We confirmed and extended these observations using several different markers of lysosomes or late endosomes, and we assessed the interactions of *Y. pestis*-containing phagosomes with the lysosomal compartment at different stages of the infection process. Our results indicate that the majority of phagosomes containing *Y. pestis* had fused with preexisiting lysosomes in macrophages after 1.5 h of infection (Fig. 2, 3, and 4A). We believe that the majority of phagosomes that we scored at this time contained viable bacteria, since there was not a substantial decrease in bacterial viability between 0.5 and 1.5 h after infection (Fig. 1A). Our results also suggested that phagosomes containing viable *Y. pestis* are not rapidly secluded from the endocytic pathway, since such phagosomes contained Lamp1 and cathepsin D after 8 h of infection (Fig. 4B). It appears that *Y. pestis*-containing phagosomes remain competent for fusion with lysosomes for at least 5 h postinfection, since BSA-gold particles pinocytosed at this time could be detected in the majority of phagosomes several hours later (Fig. 5). We believe that the formation of a spacious vacuole, as observed for about one-half of the *Y. pestis*-containing phagosomes after 8 h of infection (Fig. 5), was responsible for the low percentage of phagosomes that stained positive for newly endocytosed TROv at this time (Fig. 4B). Since formation of spacious phagosomes appeared to require bacterial viability (data not shown), it is possible that *Y. pestis* actively modifies its vacuole to enlarge it. The formation of spacious phagosomes coincides temporally with the onset of bacterial replication, which begins between 5 and 8 h postinfection (57). Although superficially the *Y. pestis*-containing phagosome appears to acquire some characteristics of a phagolysosome, it is still not known to what extent this vacuole acidifies. Furthermore, since the antibody to cathepsin D that we used does not distinguish between the immature form and the processed form of this protease, it is not clear whether the *Y. pestis*-containing phagosome completely matures into a degradative compartment. If *Y. pestis* is able to prevent complete acidification of its vacuole, as has been reported for *Yersinia pseudotuberculosis* (68), it may be able to prevent maturation of its vacuole into a phagolysosome. This process, combined with the formation of a spacious vacuole, may result in a unique intracellular niche that is favorable for replication of *Y. pestis*.

We previously described results which suggested that PhoP was important for *Y. pestis* to prevent delivery of cathepsin D to its vacuole in macrophages (25). In the present study we discovered that the permeabilization conditions used previously (0.2% Triton X-100 for 10 min) (25) for immunodetection result in extraction of cathepsin D from lysosomes and

preferential retention of cathepsin D in dead or dying bacteria in phagosomes (unpublished data). Using different conditions for permeabilization (ice-cold methanol for 30 s) that minimize extraction of cathepsin D from lysosomes, we observed here that vacuoles containing $phoP^+$ *Y. pestis* and vacuoles containing *phoP* mutant *Y. pestis* acquire cathepsin D to similar extents (Fig. 4A). In addition, phagosomes containing $phoP^+$ *Y. pestis* and phagosomes containing *phoP* mutant *Y. pestis* acquire BSA-gold particles, Lamp1, and TROv to similar extents (Fig. 3 and 4A). Therefore, we concluded that PhoP promotes intracellular survival of *Y. pestis* not by modifying phagosome trafficking but rather by promoting adaptation to the hostile environment of the vacuole. Thus, the intracellular survival strategy of *Y. pestis* differs from that of *S. enterica* serovar Typhimurium in that PhoP is not required for diversion of the vacuole from the endocytic pathway (22).

PhoP-regulated genes important for survival of *Y. pestis* in macrophages were identified by Tn5-*lacZ* mutagenesis and microarray analysis. Our approach involved overexpression of PhoP to activate gene expression (42). Of the 13 independent Tn5-*lacZ* insertion mutants that were PhoP regulated, 6 were in or near homologs of PhoP-regulated genes in *S. enterica* serovar Typhimurium (Table 2). Three of these genes were important for survival in macrophages (*mgtC*, *pmrK*, and *ugd*), while three were not (*spiR*, *pagP*, and *somA*). Microarray analysis of *Y. pestis* gene expression confirmed that *phoP* was highly overexpressed under the conditions used and revealed that a good percentage of the genes discovered in the screen (6 of 13 genes) were significantly upregulated in response to *phoP* overexpression (Table 3). Two genes identified in the screen that are homologous to PhoP-regulated genes in *S. enterica* serovar Typhimurium (*mgtC* and *pagP*) were not found to be significantly upregulated in our microarray analysis. Analysis by semiquantitative reverse transcription-PCR showed that only very small amounts of the *mgtC* transcript were present in RNA preparations of PhoP-overexpressing bacteria (Fukuto, unpublished data), which could make it difficult to detect changes in the transcript level of this gene by microarray analysis. It is also possible that the microarray oligonucleotide designed for the *mgtC* ORF does not hybridize efficiently with the *mgtC* message. The latter possibility seems likely, given that Zhou et al. identified *mgtC* and *pagP* as PhoP-regulated genes in *Y. pestis* using spotted ORF microarrays (73). In the case of *pagP*, PhoP-dependent regulation of this gene was observed when an array analysis was performed using $phoP^+$ and *phoP* mutant KIM6+ *Y. pestis* strains (see Table S4 in the supplemental material), indicating that this gene is subject to regulation by PhoP in *Y. pestis*. It is not clear why the same was not true under PhoP overexpression conditions.

In *S. enterica* serovar Typhimurium, homologs of the *mgtC* and *ugd* genes are important for adaptation to low-Mg^{2+} conditions and for in vitro resistance to antimicrobial peptides, respectively. Viable count assays performed with *Y. pestis*-infected macrophages showed that the viability of *mgtC* and *ugd* mutants decreased within 5 h after infection, indicating that both of these genes promote bacterial survival early during the infection process (Fig. 7). However, the intracellular survival phenotypes of the mutants were different, and the *ugd* mutant appeared to be more sensitive to intracellular killing at early times than the *mgtC* mutant was (Fig. 7). In contrast, *ugd*

mutant bacteria that survived the initial killing phase were able to replicate to a greater extent between 8 and 24 h than *mgtC* mutant bacteria were (Fig. 7). A *pmrF* mutant (Table 1) had an intracellular phenotype similar to that of the *ugd* mutant (data not shown), which further suggests that the behavior of the *ugd* mutant within macrophages is related to a defect in addition of aminoarabinose to lipid A. The intracellular survival phenotype of the *ugd mgtC* double mutant was more severe than the intracellular survival phenotype of either of the single mutants, indicating that these genes act by distinct mechanisms to promote intracellular survival of *Y. pestis* (Fig. 7). Taken together, these results suggest that within the first few hours of infection *Y. pestis* experiences a phagosomal environment that is replete with antimicrobial peptides but limiting for Mg^{2+}. Expression of *ugd* was upregulated several hours after *Y. pestis* was internalized within macrophage phagosomes, as shown by placing a GFP reporter under control of the *ugd* promoter (Fig. 6). Thus, *Y. pestis* must encounter environmental signals (e.g., low pH, antimicrobial peptides, or low Mg^{2+} concentration) that activate PhoP within the phagosome.

MgtC-like proteins are present in a number of intracellular pathogens (7), and for *S. enterica* serovar Typhimurium, *Brucella suis*, and *Mycobacterium tuberculosis* these proteins are important for growth in low-Mg^{2+} medium and in macrophages (6, 9, 41). MgtC is predicted to be an inner membrane protein in *S. enterica* serovar Typhimurium, but its function is not known. MgtC does not appear to be an Mg^{2+} transporter, and MgtC is not required for membrane insertion or the Mg^{2+} transport function of MgtB (48). Studies with *mgtC* mutants of *S. enterica* serovar Typhimurium, *B. suis*, and *M. tuberculosis* have suggested that a low Mg^{2+} level in phagosomes is responsible for the survival defect of these mutant bacteria. For example, addition of excess Mg^{2+} to the tissue culture medium for infected macrophages could partially rescue the survival defect of *mgtC* mutants of *S. enterica* serovar Typhimurium and *B. suis* (6, 41). In contrast to these observations, a recent study reported that the concentration of Mg^{2+} in phagosomes containing *S. enterica* serovar Typhimurium remains around 1 mM for up to 2 h postinfection (53). Mg^{2+} concentrations less than 60 μM are required to inhibit growth of an *S. enterica* serovar Typhimurium *mgtC* mutant in vitro (41). It is possible that the phagosomal concentration of Mg^{2+} drops below the threshold at times after 2 h or that an Mg^{2+} concentration of 1 mM inhibits the growth of an *mgtC* mutant in phagosomes.

Baker et al. showed that *S. enterica* serovar Typhi requires *pmrK* (also known as *pqaB*) for growth in phorbol myristate acetate-activated human macrophage-like U937 cells (3). Similarly, a cathelicidin-related antimicrobial peptide (CRAMP) produced by murine macrophages has been shown to be important for restricting growth of intracellular *S. enterica* serovar Typhimurium in macrophages (63). The same workers also found that increased resistance to CRAMP in *S. enterica* serovar Typhimurium is PhoP dependent. Therefore, it is likely that the decreased viability of *ugd* and *pmrK* mutant *Y. pestis* strains in macrophages is due to killing mechanisms involving antimicrobial peptides. As the *Y. pestis* vacuole ages, the concentration of antimicrobial peptides may decrease below a threshold level, possibly due to the formation of spacious phagosomes, which would allow replication of *ugd* mutant bac-

teria. Alternatively, other mechanisms of antimicrobial peptide resistance that are expressed at later times may compensate for the loss of *ugd*.

It is interesting that two genes identified in the screen, *pagP* and *somA*, were not important for survival of *Y. pestis* in macrophages as these genes are involved in resistance of *S. enterica* serovar Typhimurium to antimicrobial peptides. PagP modifies lipid A through addition of palmitate (C16:0), resulting in heptaacylated lipid A in *S. enterica* serovar Typhimurium (29). The additional acyl chain decreases the permeability of the outer membrane and therefore reduces the accessibility of the cytoplasmic membrane to antimicrobial peptides. To our knowledge, it has not been shown that PagP is important for survival of *S. enterica* serovar Typhimurium in macrophages, but a related gene found in *Legionella pneumophila*, *rcp*, is important for resistance to antimicrobial peptides and intracellular infection by this bacterium (62). Based on this conserved function across species, we suspect that the PagP-like protein in *Y. pestis* behaves similarly. However, it is not clear that acylation of lipid A occurs in *Y. pestis*. Rebeil et al. did not observe significant differences in lipid A acylation between *phoP*+ and *phoP* mutant *Y. pestis* strains under PhoP-inducing conditions (61). In addition, limited amounts of C16:0 were detected in lipid A from *phoP*+ *Y. pestis* under the experimental conditions used by these workers, which resulted in PhoP-dependent modification of lipid A with aminoarabinose (61). The *somA* gene confers increased resistance to polymyxin B in *S. enterica* serovar Typhimurium through an unknown mechanism and is positively regulated by PhoP inside macrophages (16). An *S. enterica* serovar Typhimurium *somA* mutant survives normally in nonactivated macrophages but is defective for systemic infection of mice (16). Interestingly, *S. enterica* serovar Typhimurium contains another PhoP-regulated gene, *virK*, which exhibits homology with *somA* and, like *somA*, promotes resistance to antimicrobial peptides and systemic virulence in mice (8). An *S. enterica* serovar Typhimurium *virK* mutant is selectively defective for survival in activated macrophages as a result of increased production of antimicrobial peptides in these cells (8). In this context, it is possible that the *Y. pestis somA* mutant could have a defective survival phenotype if activated macrophages were used in the assay. Alternatively, *somA* may encode an antimicrobial peptide resistance mechanism that is redundant to the mechanism encoded by *ugd* and the *pmr* operon. In this case, *somA* would be required for survival and growth of *ugd* mutant *Y. pestis* between 8 and 24 h postinfection (Fig. 7). Analysis of *somA ugd* double mutants in a macrophage survival assay could be used to examine this possibility.

A third PhoP-regulated gene identified in the genetic screen that was not required for survival of *Y. pestis* is y0513, which is a homolog of *spiR* (31, 51). The SpiR function is important for replication of *S. enterica* serovar Typhimurium in macrophages (32), and SpiR functions in this context as a sensor kinase to regulate expression of TTSS genes in SPI-2 (30). The observation that insertions in y0513 did not decrease the intracellular survival of *Y. pestis* is consistent with our previous data which indicated that the SPI-2-related chromosomal TTSS in *Y. pestis* is not required for replication in macrophages (57). Interestingly, microarray analysis indicated that expression of y0513 mRNA was not significantly upregulated under PhoP

overexpression conditions (data not shown). Recently, Bijlsma and Groisman obtained evidence that PhoP controls production of SpiR at the posttranscriptional level (4). These authors suggested that PhoP indirectly controls the stability or translation of *spiR* mRNA (4). If the same mechanism operates in *Y. pestis*, the promoterless *lacZ* element inserted into y0513 as a transcriptional fusion would also be subjected to the same posttranscriptional regulation.

In conclusion, here we present evidence that *Y. pestis* utilizes a set of PhoP-regulated genes that are conserved in *S. enterica* serovar Typhimurium to promote intracellular survival in macrophages. However, the trafficking of the *Y. pestis*-containing phagosome is clearly distinct from the trafficking observed for *S. enterica* serovar Typhimurium, as *Y. pestis* survives and replicates in a phagosome that fuses with lysosomes and does not become secluded from the endocytic pathway for up to 8 h postinfection. Additional studies are needed to better characterize the trafficking of the *Y. pestis*-containing phagosome and should include experiments that look at later infection times than those used here. In addition, because *Y. pestis* inhabits an intracellular niche that appears to be different from the niche inhabited by *S. enterica* serovar Typhimurium, it is quite likely that a set of novel genes required for this process is present in *Y. pestis*. Further use of genetic and microarray approaches should be fruitful for identification of these factors.

REFERENCES

1. **Alexeyev, M. F.** 1995. Three kanamycin resistance gene cassettes with different polylinkers. BioTechniques **18:**52, 54, 56.
2. **Bader, M. W., S. Sanowar, M. E. Daley, A. R. Schneider, U. Cho, W. Xu, R. E. Klevit, H. Le Moual, and S. I. Miller.** 2005. Recognition of antimicrobial peptides by a bacterial sensor kinase. Cell **122:**461–472.
3. **Baker, S. J., J. S. Gunn, and R. Morona.** 1999. The *Salmonella typhi* melittin resistance gene *pqaB* affects intracellular growth in PMA-differentiated U937 cells, polymyxin B resistance and lipopolysaccharide. Microbiology **145:**367–378.
4. **Bijlsma, J. J., and E. A. Groisman.** 2005. The PhoP/PhoQ system controls the intramacrophage type three secretion system of *Salmonella enterica*. Mol. Microbiol. **57:**85–96.
5. **Black, D. S., and J. B. Bliska.** 2000. The RhoGAP activity of the *Yersinia pseudotuberculosis* cytotoxin YopE is required for antiphagocytic function and virulence. Mol. Microbiol. **37:**515–527.
6. **Blanc-Potard, A. B., and E. A. Groisman.** 1997. The *Salmonella selC* locus contains a pathogenicity island mediating intramacrophage survival. EMBO J. **16:**5376–5385.
7. **Blanc-Potard, A. B., and B. Lafay.** 2003. MgtC as a horizontally-acquired virulence factor of intracellular bacterial pathogens: evidence from molecular phylogeny and comparative genomics. J. Mol. Evol. **57:**479–486.
8. **Brodsky, I. E., N. Ghori, S. Falkow, and D. Monack.** 2005. Mig-14 is an inner membrane-associated protein that promotes *Salmonella typhimurium* resistance to CRAMP, survival within activated macrophages and persistent infection. Mol. Microbiol. **55:**954–972.
9. **Buchmeier, N., A. Blanc-Potard, S. Ehrt, D. Piddington, L. Riley, and E. A.**

Groisman. 2000. A parallel intraphagosomal survival strategy shared by *Mycobacterium tuberculosis* and *Salmonella enterica*. Mol. Microbiol. **35:**1375–1382.

10. **Buchmeier, N. A., and F. Heffron.** 1991. Inhibition of macrophage phago-some-lysosome fusion by *Salmonella typhimurium*. Infect. Immun. **59:**2232–2238.

11. **Cavanaugh, D. C., and R. Randall.** 1959. The role of multiplication of *Pasteurella pestis* in mononuclear phagocytes in the pathogenesis of fleaborne plague. J. Immunol. **85:**348–363.

12. **Charnetzky, W. T., and W. W. Shuford.** 1985. Survival and growth of *Yersinia pestis* within macrophages and an effect of the loss of the 47-megadalton plasmid on growth in macrophages. Infect. Immun. **47:**234–241.

13. **Conchas, R. F., and E. Carniel.** 1990. Highly efficient electroporation of *Yersinia*. Gene **87:**133–137.

14. **Cuellar-Mata, P., N. Jabado, J. Liu, W. Furuya, B. B. Finlay, P. Gros, and S. Grinstein.** 2002. Nramp1 modifies the fusion of *Salmonella typhimurium*-containing vacuoles with cellular endomembranes in macrophages. J. Biol. Chem. **277:**2258–2265.

15. **Deng, W., V. Burland, G. Plunkett, 3rd, A. Boutin, G. F. Mayhew, P. Liss, N. T. Perna, D. J. Rose, B. Mau, S. Zhou, D. C. Schwartz, J. D. Fetherston, L. E. Lindler, R. R. Brubaker, G. V. Plano, S. C. Straley, K. A. McDonough, M. L. Nilles, J. S. Matson, F. R. Blattner, and R. D. Perry.** 2002. Genome sequence of *Yersinia pestis* KIM. J. Bacteriol. **184:**4601–4611.

16. **Detweiler, C. S., D. M. Monack, I. E. Brodsky, H. Mathew, and S. Falkow.** 2003. *virK*, *somA* and *rcsC* are important for systemic *Salmonella enterica* serovar Typhimurium infection and cationic peptide resistance. Mol. Microbiol. **48:**385–400.

17. **Du, Y., R. Rosqvist, and A. Forsberg.** 2002. Role of fraction 1 antigen of *Yersinia pestis* in inhibition of phagocytosis. Infect. Immun. **70:**1453–1460.

18. **Duclos, S., and M. Desjardins.** 2000. Subversion of a young phagosome: the survival strategies of intracellular pathogens. Cell. Microbiol. **2:**365–377.

19. **Ernst, R. K., T. Guina, and S. I. Miller.** 1999. How intracellular bacteria survive: surface modifications that promote resistance to host innate immune responses. J. Infect. Dis. **179:**S326–S330.

20. **Fetherston, J. D., P. Schuetze, and R. D. Perry.** 1992. Loss of the pigmen-tation phenotype in *Yersinia pestis* is due to the spontaneous deletion of 102 kb of chromosomal DNA which is flanked by a repetitive element. Mol. Microbiol. **6:**2693–2704.

21. **Finegold, M. J.** 1969. Pneumonic plague in monkeys. An electron micro-scopic study. Am. J. Pathol. **54:**167–185.

22. **Garvis, S. G., C. R. Beuzon, and D. W. Holden.** 2001. A role for the PhoP/Q regulon in inhibition of fusion between lysosomes and *Salmonella*-containing vacuoles in macrophages. Cell. Microbiol. **3:**731–744.

23. **Gentleman, R. C., V. J. Carey, D. M. Bates, B. Bolstad, M. Dettling, S. Dudoit, B. Ellis, L. Gautier, Y. Ge, J. Gentry, K. Hornik, T. Hothorn, W. Huber, S. Iacus, R. Irizarry, F. Leisch, C. Li, M. Maechler, A. J. Rossini, G. Sawitzki, C. Smith, G. Smyth, L. Tierney, J. Y. Yang, and J. Zhang.** 2004. Bioconductor: open software development for computational biology and bioinformatics. Genome Biol. **5:**R80.

24. **Gong, S., S. W. Bearden, V. A. Geoffroy, J. D. Fetherston, and R. D. Perry.** 2001. Characterization of the *Yersinia pestis* Yfu ABC inorganic iron trans-port system. Infect. Immun. **69:**2829–2837.

25. **Grabenstein, J. P., M. Marceau, C. Pujol, M. Simonet, and J. B. Bliska.** 2004. The response regulator PhoP of *Yersinia pseudotuberculosis* is impor-tant for replication in macrophages and for virulence. Infect. Immun. **72:**4973–4984.

26. **Groisman, E. A.** 2001. The pleiotropic two-component regulatory system PhoP-PhoQ. J. Bacteriol. **183:**1835–1842.

27. **Gunn, J. S., K. B. Lim, J. Krueger, K. Kim, L. Guo, M. Hackett, and S. I. Miller.** 1998. PmrA-PmrB-regulated genes necessary for 4-aminoarabinose lipid A modification and polymyxin resistance. Mol. Microbiol. **27:**1171–1182.

28. **Guo, L., K. B. Lim, J. S. Gunn, B. Bainbridge, R. P. Darveau, M. Hackett, and S. I. Miller.** 1997. Regulation of lipid A modifications by *Salmonella typhimurium* virulence genes *phoP-phoQ*. Science **276:**250–253.

29. **Guo, L., K. B. Lim, C. M. Poduje, M. Daniel, J. S. Gunn, M. Hackett, and S. I. Miller.** 1998. Lipid A acylation and bacterial resistance against verte-brate antimicrobial peptides. Cell **95:**189–198.

30. **Hensel, M.** 2000. *Salmonella* pathogenicity island 2. Mol. Microbiol. **36:**1015–1023.

31. **Hensel, M., J. E. Shea, B. Raupach, D. Monack, S. Falkow, C. Gleeson, T. Kubo, and D. W. Holden.** 1997. Functional analysis of *ssaJ* and the *ssaK/U* operon, 13 genes encoding components of the type III secretion apparatus of *Salmonella* pathogenicity island 2. Mol. Microbiol. **24:**155–167.

32. **Hensel, M., J. E. Shea, S. R. Waterman, R. Mundy, T. Nikolaus, G. Banks, A. Vazquez-Torres, C. Gleeson, F. C. Fang, and D. W. Holden.** 1998. Genes encoding putative effector proteins of the type III secretion system of *Sal-monella* pathogenicity island 2 are required for bacterial virulence and pro-liferation in macrophages. Mol. Microbiol. **30:**163–174.

33. **Hitchen, P. G., J. L. Prior, P. C. Oyston, M. Panico, B. W. Wren, R. W. Titball, H. R. Morris, and A. Dell.** 2002. Structural characterization of lipo-oligosaccharide (LOS) from *Yersinia pestis*: regulation of LOS structure by the PhoPQ system. Mol. Microbiol. **44:**1637–1650.

34. **Hmiel, S. P., M. D. Snavely, J. B. Florer, M. E. Maguire, and C. G. Miller.** 1989. Magnesium transport in *Salmonella typhimurium*: genetic character-ization and cloning of three magnesium transport loci. J. Bacteriol. **171:**4742–4751.

35. **Holden, D. W.** 2002. Trafficking of the *Salmonella* vacuole in macrophages. Traffic **3:**161–169.

36. **Inglesby, T. V., D. T. Dennis, D. A. Henderson, J. G. Bartlett, M. S. Ascher, E. Eitzen, A. D. Fine, A. M. Friedlander, J. Hauer, J. F. Koerner, M. Layton, J. McDade, M. T. Osterholm, T. O'Toole, G. Parker, T. M. Perl, P. K. Russell, M. Schoch-Spana, and K. Tonat.** 2000. Plague as a biological weap-on: medical and public health management. Working Group on Civilian Biodefense. JAMA **283:**2281–2290.

37. **Janssen, W. A., and M. J. Surgalla.** 1968. Plague bacillus: survival within host phagocytes. Science **163:**950–952.

38. **Kent, W. J.** 2002. BLAT—the BLAST-like alignment tool. Genome Res. **12:**656–664.

39. **Knodler, L. A., and O. Steele-Mortimer.** 2003. Taking possession: biogenesis of the *Salmonella*-containing vacuole. Traffic **4:**587–599.

40. **Lathem, W. W., S. D. Crosby, V. L. Miller, and W. E. Goldman.** 2005. Progression of primary pneumonic plague: a mouse model of infection, pathology, and bacterial transcriptional activity. Proc. Natl. Acad. Sci. USA **102:**17786–17791.

41. **Lavigne, J. P., D. O'Callaghan, and A. B. Blanc-Potard.** 2005. Requirement of MgtC for *Brucella suis* intramacrophage growth: a potential mechanism shared by *Salmonella enterica* and *Mycobacterium tuberculosis* for adaptation to a low-Mg^{2+} environment. Infect. Immun. **73:**3160–3163.

42. **Lejona, S., M. E. Castelli, M. L. Cabeza, L. J. Kenney, E. Garcia Vescovi, and F. C. Soncini.** 2004. PhoP can activate its target genes in a PhoQ-independent manner. J. Bacteriol. **186:**2476–2480.

43. **Lukaszewski, R. A., D. J. Kenny, R. Taylor, D. G. Rees, M. G. Hartley, and P. C. Oyston.** 2005. Pathogenesis of *Yersinia pestis* infection in BALB/c mice: effects on host macrophages and neutrophils. Infect. Immun. **73:**7142–7150.

44. **Marceau, M., F. Sebbane, F. Ewann, F. Collyn, B. Lindner, M. A. Campos, J. A. Bengoechea, and M. Simonet.** 2004. The *pmrF* polymyxin-resistance operon of *Yersinia pseudotuberculosis* is upregulated by the PhoP-PhoQ two-component system but not by PmrA-PmrB, and is not required for virulence. Microbiology **150:**3947–3957.

45. **Meyer, K. F.** 1950. Immunity in plague; a critical consideration of some recent studies. J. Immunol. **64:**139–163.

46. **Miller, J. H.** 1992. A short course in bacterial genetics: a laboratory manual and handbook for *Escherichia coli* and related bacteria. Cold Spring Harbor Laboratory Press, Cold Spring Harbor, N.Y.

47. **Mills, S. D., and B. B. Finlay.** 1998. Isolation and characterization of *Sal-monella typhimurium* and *Yersinia pseudotuberculosis*-containing phagosomes from infected mouse macrophages: *Y. pseudotuberculosis* traffics to terminal lysosomes where they are degraded. Eur. J. Cell Biol. **77:**35–47.

48. **Moncrief, M. B., and M. E. Maguire.** 1998. Magnesium and the role of MgtC in growth of *Salmonella typhimurium*. Infect. Immun. **66:**3802–3809.

49. **Morales, V. M., A. Backman, and M. Bagdasarian.** 1991. A series of wide-host-range low-copy-number vectors that allow direct screening for recom-binants. Gene **97:**39–47.

50. **Nummila, K., I. Kilpelainen, U. Zahringer, M. Vaara, and I. M. Helander.** 1995. Lipopolysaccharides of polymyxin B-resistant mutants of *Escherichia coli* are extensively substituted by 2-aminoethyl pyrophosphate and contain aminoarabinose in lipid A. Mol. Microbiol. **16:**271–278.

51. **Ochman, H., F. C. Soncini, F. Solomon, and E. A. Groisman.** 1996. Identi-fication of a pathogenicity island required for *Salmonella* survival in host cells. Proc. Natl. Acad. Sci. USA **93:**7800–7804.

52. **Oh, Y. K., C. Alpuche-Aranda, E. Berthiaume, T. Jinks, S. I. Miller, and J. A. Swanson.** 1996. Rapid and complete fusion of macrophage lysosomes with phagosomes containing *Salmonella typhimurium*. Infect. Immun. **64:**3877–3883.

53. **Orozco, N. M., N. Touret, M. L. Zaharik, E. Park, R. Kopelman, S. Miller, B. B. Finlay, P. Gros, and S. Grinstein.** 2005. Visualization of vacuolar acidification-induced transcription of genes of pathogens inside macro-phages. Mol. Biol. Cell **17:**498–510.

54. **Oyston, P. C. F., N. Dorrell, K. Williams, S.-R. Li, M. Green, R. W. Titball, and B. Wren.** 2000. The response regulator PhoP is important for survival under conditions of macrophage-induced stress and virulence in *Yersinia pestis*. Infect. Immun. **68:**3419–3425.

55. **Parkhill, J., B. W. Wren, N. R. Thomson, R. W. Titball, M. T. Holden, M. B. Prentice, M. Sebaihia, K. D. James, C. Churcher, K. L. Mungall, S. Baker, D. Basham, S. D. Bentley, K. Brooks, A. M. Cerdeno-Tarraga, T. Chilling-worth, A. Cronin, R. M. Davies, P. Davis, G. Dougan, T. Feltwell, N. Hamlin, S. Holroyd, K. Jagels, A. V. Karlyshev, S. Leather, S. Moule, P. C. Oyston, M. Quail, K. Rutherford, M. Simmonds, J. Skelton, K. Stevens, S. White-head, and B. G. Barrell.** 2001. Genome sequence of *Yersinia pestis*, the causative agent of plague. Nature **413:**523–527.

56. **Perry, R. D., and J. D. Fetherston.** 1997. *Yersinia pestis*—etiologic agent of plague. Clin. Microbiol. Rev. **10:**35–66.

57. **Pujol, C., and J. B. Bliska.** 2003. The ability to replicate in macrophages is conserved between *Yersinia pestis* and *Yersinia pseudotuberculosis*. Infect. Immun. **71:**5892–5899.

58. **Pujol, C., and J. B. Bliska.** 2004. Turning *Yersinia* pathogenesis outside in: subversion of macrophage function by intracellular yersiniae. Clin. Immunol. **114:**216–226.

59. **Pujol, C., J. P. Grabenstein, R. D. Perry, and J. B. Bliska.** 2005. Replication of *Yersinia pestis* in interferon gamma-activated macrophages requires *ripA*, a gene encoded in the pigmentation locus. Proc. Natl. Acad. Sci. USA **102:**12909–12914.

60. **Rathman, M. R., and S. Falkow.** 1997. The unique trafficking pattern of *Salmonella typhimurium*-containing phagosomes in murine macrophages is independent of the mechanism of bacterial entry. Infect. Immun. **65:**1475–1485.

61. **Rebeil, R., R. K. Ernst, B. B. Gowen, S. I. Miller, and B. J. Hinnebusch.** 2004. Variation in lipid A structure in the pathogenic yersiniae. Mol. Microbiol. **52:**1363–1373.

62. **Robey, M., W. O'Connell, and N. P. Cianciotto.** 2001. Identification of *Legionella pneumophila rcp*, a *pagP*-like gene that confers resistance to cationic antimicrobial peptides and promotes intracellular infection. Infect. Immun. **69:**4276–4286.

63. **Rosenberger, C. M., R. L. Gallo, and B. B. Finlay.** 2004. Interplay between antibacterial effectors: a macrophage antimicrobial peptide impairs intracellular *Salmonella* replication. Proc. Natl. Acad. Sci. USA **101:**2422–2427.

64. **Sebbane, F., D. Gardner, D. Long, B. B. Gowen, and B. J. Hinnebusch.** 2005. Kinetics of disease progression and host response in a rat model of bubonic plague. Am. J. Pathol. **166:**1427–1439.

65. **Smyth, G. K.** 2004. Linear models and empirical Bayes methods for assessing differential expression in microarray experiments. Stat. Applic. Genet. Mol. Biol. **3:**article 3. [Online.] http://www.bepress.com/sagmb/vol3/iss1/art3/.

66. **Straley, S. C., and P. A. Harmon.** 1984. Growth in mouse peritoneal macrophages of *Yersinia pestis* lacking established virulence determinants. Infect. Immun. **45:**649–654.

67. **Straley, S. C., and P. A. Harmon.** 1984. *Yersinia pestis* grows within phagolysosomes in mouse peritoneal macrophages. Infect. Immun. **45:**655–659.

68. **Tsukano, H., F. Kura, S. Inoue, S. Sato, H. Izumiya, T. Yasuda, and H. Watanabe.** 1999. *Yersinia pseudotuberculosis* blocks the phagosomal acidification of B10.A mouse macrophages through the inhibition of vacuolar H^+-ATPase activity. Microb. Pathog. **27:**253–263.

69. **Viboud, G. I., and J. B. Bliska.** 2005. *Yersinia* outer proteins: role in modulation of host cell signaling responses and pathogenesis. Annu. Rev. Microbiol. **59:**69–89.

70. **Welkos, S., M. L. M. Pitt, M. Martinez, A. Friedlander, P. Vogel, and R. Tammariello.** 2002. Determination of the virulence of the pigmentation-deficient and pigmentation-/plasminogen activator-deficient strains of *Yersinia pestis* in non-human primate and mouse models of pneumonic plague. Vaccine **20:**2206–2214.

71. **Welkos, S. L., A. M. Friedlander, and K. J. Davis.** 1997. Studies on the role of plasminogen activator in systemic infection by virulent *Yersinia pestis* strain CO92. Microb. Pathog. **23:**211–223.

72. **Winfield, M. D., T. Latifi, and E. A. Groisman.** 2005. Transcriptional regulation of the 4-amino-4-deoxy-L-arabinose biosynthetic genes in *Yersinia pestis*. J. Biol. Chem. **280:**14765–14772.

73. **Zhou, D., Y. Han, L. Qin, Z. Chen, J. Qiu, Y. Song, B. Li, J. Wang, Z. Guo, Z. Du, X. Wang, and R. Yang.** 2005. Transcriptome analysis of the Mg^{2+}-responsive PhoP regulator in *Yersinia pestis*. FEMS Microbiol. Lett. **250:** 85–95.